

Article

## Using Nighttime Satellite Imagery as a Proxy Measure of Human Well-Being

Tilottama Ghosh <sup>1,\*</sup>, Sharolyn J. Anderson <sup>2</sup>, Christopher D. Elvidge <sup>3</sup> and Paul C. Sutton <sup>2,4</sup>

<sup>1</sup> Cooperative Institute for Research in the Environmental Sciences, University of Colorado, Boulder, CO 80309, USA

<sup>2</sup> School of Natural and Built Environments and The Barbara Hardy Institute, University of South Australia, Adelaide 5001, Australia; E-Mails: sharolyn.anderson@unisa.edu.au (S.J.N.); paul.sutton@unisa.edu.au (P.C.S.)

<sup>3</sup> NOAA National Geophysical Data Center, Boulder, CO 80305, USA; E-Mail: chris.elvidge@noaa.gov

<sup>4</sup> Department of Geography, University of Denver, Denver, CO 80208, USA

\* Author to whom correspondence should be addressed; E-Mails: tilottama.ghosh@noaa.gov or ghoshtilottama@hotmail.com; Tel.: +91-8826860007.

*Received: 23 September 2013; in revised form: 8 October 2013 / Accepted: 4 November 2013 /*

*Published: 26 November 2013*

---

**Abstract:** Improving human well-being is increasingly recognized as essential for movement toward a sustainable and desirable future. Estimates of different aspects of human well-being, such as Gross Domestic Product, or percentage of population with access to electric power, or measuring the distribution of income in society are often fraught with problems. There are few standardized methods of data collection; in addition, the required data is not obtained in a reliable manner and on a repetitive basis in many parts of the world. Consequently, inter-comparability of the data that does exist becomes problematic. Data derived from nighttime satellite imagery has helped develop various globally consistent proxy measures of human well-being at the gridded, sub-national, and national level. We review several ways in which nighttime satellite imagery has been used to measure the human well-being within nations.

**Keywords:** nighttime lights imagery; LandScan population data; human well-being; Night Light Development Index (NLDI); Gross Domestic Product; informal economy; poverty rates; electrification rates; human ecological footprint

---

## 1. Introduction

Images of the “Earth at Night” derived from nighttime satellite imagery provided by the Defense Meteorological Satellite Program’s Operational Linescan System (DMSP-OLS) have become a recognizable spatially explicit global icon of human presence on the planet. Nighttime imagery has been used to develop several proxy measures of human well-being.

Gross Domestic Product (GDP), which is the monetary market value of all final goods and services produced in a country over a period of a year, is often used as an indicator for judging the relative “standard of living” of a country in comparison to other countries. GDP growth is implicitly and often explicitly recognized as a determining factor of social welfare [1].

The close relation between the spatial distribution of nighttime lights and economic activity has been observed and utilized in several studies before [2–7]. These studies have only expanded the interest of examining the spatial and temporal relationships between the spatially explicit remotely-sensed nighttime imagery and national-level GDPs or sub-national-level Gross State Products (GSPs). Current studies include the creation of a global grid of estimated economic activity at 1 km<sup>2</sup> spatial resolution [8], and probing the relationships for other countries [9–17].

Poverty-afflicted areas are associated with deprivation of not only material possessions, but also basic human needs including food, water, sanitation, clothing, shelter, health care, and education. Objective metrics of human well-being derived from nighttime imagery helps identify areas of the world in great need of improved human development. The nighttime light satellite images have also been used to examine poverty at the grid-level, as well as at the sub-national and national levels [18–21].

Questions have been raised time and again about the utility of GDP or GDP per capita as a sole measure of a country’s well-being. GDP cannot provide any guarantee about the quality of the goods and services produced in a country, or whether it adds any value to social progress or human happiness [22]. For instance, GDP does not differentiate between expenditure on good things, for example, education, and bad things, for example, alcohol, drugs, or cigarettes. GDP does not quantify work that does not have a market price attached to it, and disregards informal transactions outside markets. For instance, subsistence agriculture, voluntary work, household work, and childcare, are completely overlooked in the national accounting of GDP. Per capita GDP emphasizes average income but neglects income distribution, albeit uneven distribution of income results in unequal opportunities for personal development and well-being. GDP does not quantify the economic services provided by nature, for example, the value of forests in protecting watersheds and in the storage of carbon, or the importance of wetlands in flood protection, and protecting areas from storm surges [1].

Because of the questions raised about the validity and utility of GDP as a measure of well-being, researchers have used nighttime light images to not only quantify the economic well-being of nations, but have also estimated informal economy [23], evaluated inequality in human development (Nightlight Development Index or NLDI) [24], and have examined the anthropological impacts or “costs” inflicted by human activities on earth [25]. Measuring the anthropological impacts of human activities adds an environmental dimension to the measurement of a country’s well-being.

Two other aspects of human well-being which have been measured using nighttime light images that are discussed in this paper are—the relation of nighttime lights and electrification rates [26],

and the development of surrogate measures of the Information and Communication Technology Development Index (IDI) for determining the development of countries as information societies [27].

The nature of urban form and the patterns of urban development are regarded as having a fundamentally important impact on ecosystem function, ecosystem health, and sustainability [28]. Continuing studies of the dynamics of urbanization through time using nighttime lights enables the comprehension of adverse effects of urbanization related to loss of vegetation, increase in temperatures, air and water pollution, loss of species' habitats, growth and spread of urban slums, poverty, and unemployment. Nighttime light images have also informed studies of urban dynamics [29–32].

This paper reviews some of the recent studies in which nighttime satellite imagery has been used to measure various aspects of the human well-being of nations, with particular emphasis on some of the pioneering studies. The “Methods and Results” for each of the studies is discussed in Section 2, followed by the “Discussion” section in Section 3, and “Conclusion” in Section 4.

## **2. Methods and Results: Estimates of Various Indicators of Human Well-Being Using Nighttime Lights**

The source of all the nighttime imageries used in these studies is from the Earth Observation Group (EOG), the National Geophysical Data Center (NGDC) of the National Oceanic and Atmospheric Administration (NOAA). The EOG at NOAA has been archiving and processing Defense Meteorological Satellite Program's Operational Linescan System (DMSP-OLS) nighttime lights data since 1994. The EOG produces two types of nighttime images at approximately 1 km resolution (30 arc-seconds)—the stable light images and the radiance-calibrated images. In all of the following studies, one or both types of nighttime images have been used. The annual, global stable lights are generated by averaging the individual, cloud-free orbits of the Operation Linescan System (OLS) visible band data. In the creation of the stable lights product, fires and other ephemeral lights are removed based on their high brightness and short duration [33]. Annual stable lights images from 1992 to 2012 are available for free download from EOG's website [34]. One of the problems associated with the stable lights data is the saturation of the recorded data in the city centers because of six bit quantization and limited dynamic range.

To overcome this problem, a limited set of observations was obtained at low lunar illumination and at significantly lower gain settings for some years. The radiance-calibrated images for those years were created by combining these sparse data (fixed gain data) acquired at low gain settings with the operational data (stable lights data) acquired at high gain settings. The radiance-calibrated data are characterized by unsaturated values in the urban centers [35]. The radiance-calibrated data of 2006 is available for free download from the EOG's website [36].

Another dataset which has been used for many of these studies is the LandScan population dataset. The LandScan population data produced by the U.S. Department of Energy at Oak Ridge National Laboratory (ORNL) represents ambient population count (averaged over 24 h) at approximately 1 km<sup>2</sup> resolution (the same spatial resolution as the data products derived from the nighttime images). A progressive series of spatially disaggregated global population count datasets have been made available through the years. However, previous versions of the LandScan data are made unavailable as

new datasets are released because the makers of the LandScan data at ORNL caution against using the data as a change detection or migration tool [37].

### 2.1. Nighttime Lights and Gross Domestic Product (GDP)

Amongst the recent studies linking the spatially explicit DMSP-OLS nighttime lights data and GDP at the national level or GSP at the sub-national level has been the creation of a global grid of total economic activity [8]. This study acted as a milestone as it was the finest resolution grid of economic activity with global coverage that was ever created. Moreover, it also took into account informal economic activity, and the distribution of agricultural economic activity.

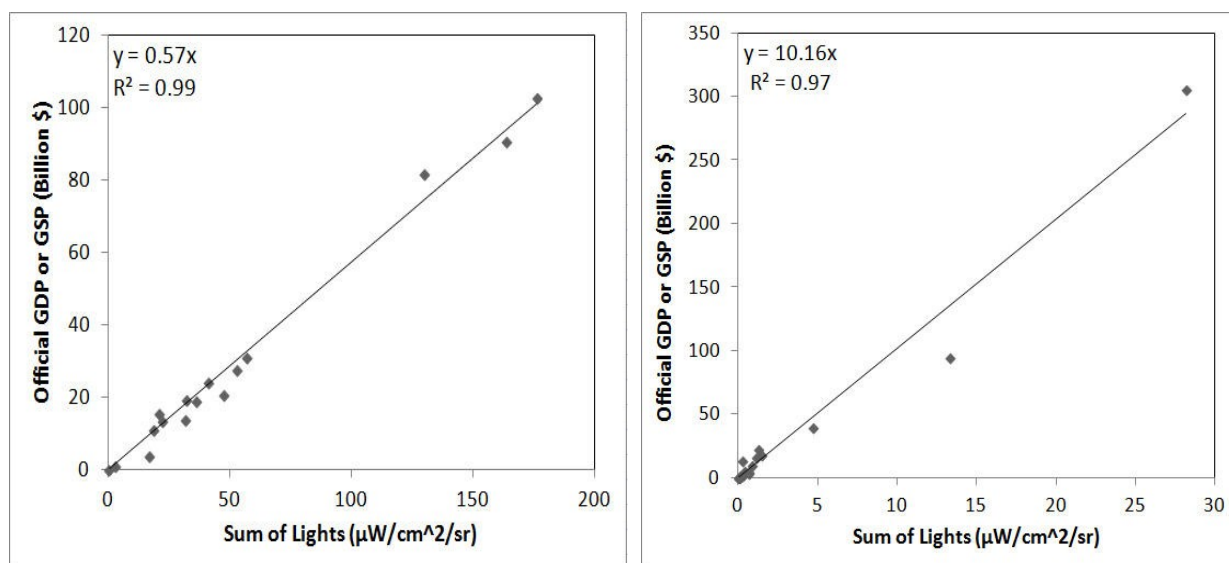
The radiance-calibrated nighttime image of 2006 and the LandScan population data of 2006 were used in this study. As a first step towards creating the disaggregated global grid of estimated total (formal plus informal) economic activity at a spatial resolution of 1 km<sup>2</sup> for states and countries of the world, sum of light (SOL) intensity values for the countries of the world and for the states of the United States (U.S.), China, Mexico, and India, were computed from the radiance-calibrated nighttime image of 2006. The SOL were computed at the sub-national level for the countries of China, India, Mexico, and the U.S. because when the SOL were regressed against the official GDP values, these countries proved to be outliers, and provided the greatest weight in increasing the  $R^2$  value. Thus, the GSPs, or in other words, GDP at the state level, were considered for these four countries, and GDP was considered for rest of the countries of the world. Ratios ( $R_i$ ) of the sum of lights ( $SL_i$ ) to the official  $GSP_i$  (Equation (1)) or  $GDP_i$  (Equation (2)) for each administrative unit were calculated as follows:

$$R_i = SL_i / GSP_i \quad (1)$$

or,

$$R_i = SL_i / GDP_i \quad (2)$$

The calculated ratios enabled the grouping of administrative units (countries and states) on the basis of their SOL values relative to their GDP or GSP values, as it was observed that administrative units may be brighter or dimmer in comparison to their levels of economic activity. This created 36 overlapping groups of administrative units such that even if each group had administrative units representing different levels of economic development, they were included in the specific range of lighting to GSP or GDP ratio. Estimates of the informal economy as a percentage of total official GDP was taken from Schneider's computations [38–40]. Regression models were developed to calibrate the SOL to the official GDP and GSP values plus informal economy for all the 36 groups, and  $R^2$  greater than 0.9 was obtained for all the groups (Figure 1).

**Figure 1.** Regression models for estimating coefficients for sample groups.

An empirical relationship was identified between the ratios of SOL and GDP or GSP for each administrative unit ( $R_i$ ), and the estimated beta coefficients across all groups ( $\beta_j$ ). This relationship was described as a natural logarithmic function between these two variables (Equation (3)) and exponentiating  $\ln(\beta_j)$  provided unique coefficients ( $\beta_i'$ ) for each of the administrative units.

$$\ln(\beta_j) = 0.58 - 0.95 \cdot \ln(R_i) \quad (3)$$

$$\beta_i' = \text{Exp}(0.58 - 0.95 \cdot \ln(R_i)) \quad (4)$$

These unique coefficients were multiplied with the SOL of each of the administrative units to derive the estimated GDP ( $GDPI_i$ ) or GSP ( $GSPI_i$ ) values (Equations (5) and (6)).

$$\beta_i' \times SL_i = GSPI_i \quad (5)$$

$$\beta_i' \times SL_i = GDPI_i \quad (6)$$

These estimated total values of economic activity were distributed using both the nighttime lights grid and the LandScan population grid of 2006. The percentage contribution of agriculture towards the total economic activity for the administrative unit was distributed according to the LandScan population grid, with the assumption that distribution of agricultural activity is associated with rural population who might not show up in the nighttime light images, but are captured in the LandScan population grid. This created the grid of agricultural economic activity. A grid of non-agricultural economic activity was created by distributing the percentage of economic activity attributed to the commercial/industrial sector on the basis of the nighttime lights. The grids of agricultural and non-agricultural economic activity were added to produce the grid of total economic activity. This resulted in a disaggregated global map of economic activity at the spatial resolution of  $1 \text{ km}^2$  pixels, with each pixel representing millions of dollars (*i.e.*,  $\text{\$Mn/km}^2$ ) (Figures 2 and 3).

**Figure 2.** Grid of total economic activity in millions of dollars per km<sup>2</sup> pixel.

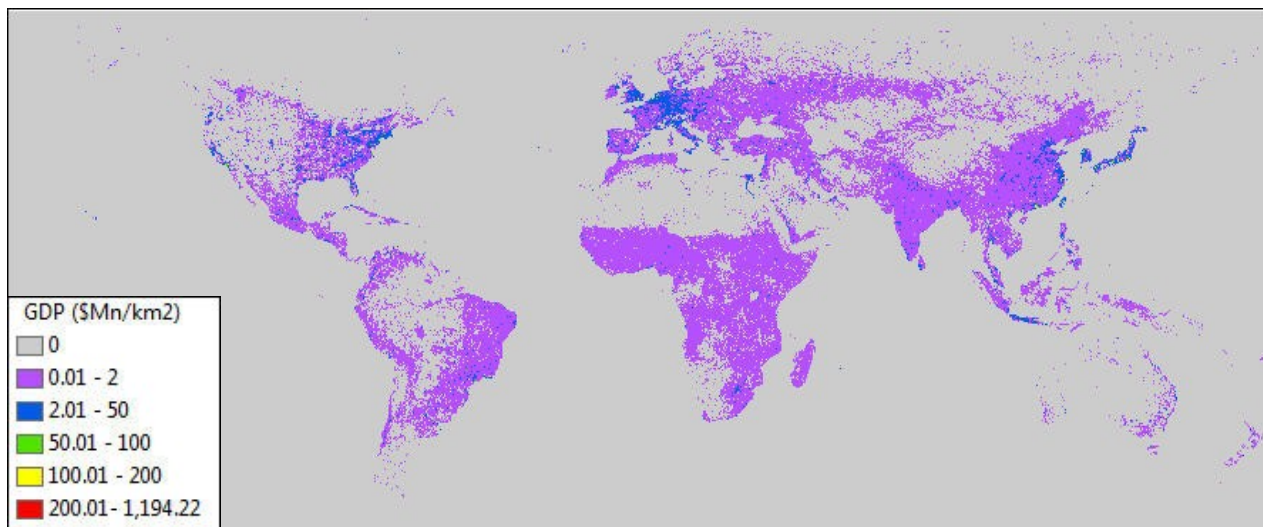
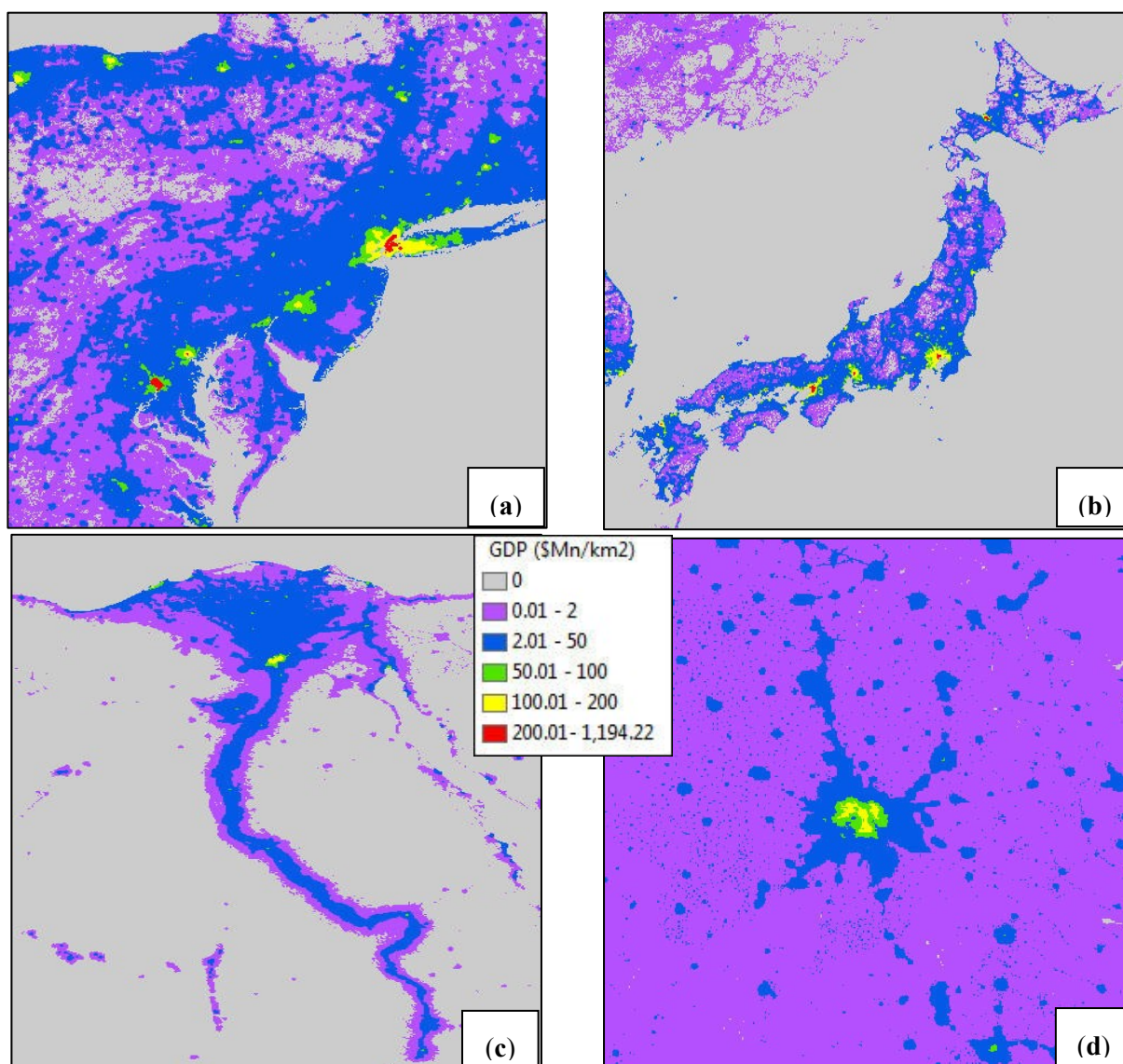


**Figure 3.** Grid of total economic activity in millions of dollars per km<sup>2</sup> pixel (a) North-eastern United States, (b) Japan, (c) Nile Delta, Egypt, (d) New Delhi, India.



The estimated GSPI<sub>i</sub> and GDPI<sub>i</sub> were aggregated to the state and the country level, respectively, and were compared to the official estimates of GSP and GDP. The estimated values were greater than official estimates by up to 30 percent for almost all the administrative units. This was as expected because the estimated values were derived through calibration of the SOL with the official GDP or GSP with the addition of an estimate of the informal economy. When compared with GDP or GSP with added informal economy percentages, it showed a mixed picture of underestimation to about 40 percent and overestimation to about 25 percent at the national and sub-national level [8].

In another landmark study three economists from Brown University put forward the significance of the nighttime lights data in measuring economic growth of countries, especially for those with low-quality income data. They developed a statistical framework to demonstrate how changes in night light data from 1992 to 2003 could be used to complement official income data to get improved estimates of true income growth of countries [12]. When the researchers applied their developed methodology to countries with low-quality income data, the derived estimates were significantly different from the official estimates. For example, while official estimates suggested a negative 2.6 percent annual growth in GDP for the Democratic Republic of Congo, lights suggested a 2.4 percent annual growth rate in GDP. Thus, lights suggested Congo as growing faster than what official estimates suggested. On the other hand, although Myanmar had an official growth rate of 8.6 percent a year, lights implied a much slower growth rate at 3.4 percent. The results obtained from the nighttime images were more believable considering the socio-economic and political situations of those countries.

Pestalozzi *et al.* [15] in their intensive analysis of the spatial distribution of lights over 17 years (1992–2009) have found that the global “center of gravity” of the nighttime lights has been moving east and south as emerging economies in India, China, and Southeast Asia have “lit up”. Further analysis of brightly lit city growth covering 160 countries demonstrated the efficacy of the nighttime light images in monitoring the expansion of developing countries (like India and Brazil), the expansion of agglomeration sizes (like Shanghai in China and the Nile delta of Egypt), the degeneration of countries undergoing a demographic decline and a reduction in urban population (like Russia and the Ukraine), and the successful implementation of light abatement programs like that of Canada and the United Kingdom.

The spatial relationship between nighttime lights and economic activity has been examined in greater depth for studies conducted in other countries. For example, Xiangdi *et al.* [14] found a clear logarithmic linear relationship between nightlight index and the sum of secondary and tertiary industry at the national level for China. They extended the relationship to create a 1km grid GDP map of China reflecting the national distribution of the secondary and tertiary industry of China at a finer spatial resolution.

Similarly, in a current study for Myanmar, the spatial relationships between nighttime light patterns and economic activity were exploited to estimate GDP at the district level, and later the relationship between spatial distributions of economic activity with population was also examined, which would have important policy implications for the country [16]. An investigation of the applicability of the DMSP-OLS data in monitoring settlement patterns, population, electricity consumption, GDP, and carbon dioxide emissions at different spatial levels for the Republic of Kazakhstan proved the value of the DMSP-OLS data in monitoring such socio-economic parameters [13].

Investigations were also conducted to estimate total GDP and sector-wise GDP (primary, secondary and tertiary sector) at a greater granular level, that is, at the district-level for developing countries like India. Log-linear models between sum of lights (SOL) and official GDP values, with dummy variables for districts with hierarchical urban clusters (metros, sub-metros, capital cities), and snow-covered areas, were developed. Through these models it was observed that nighttime lights data could explain a large part of the variation in district level GDP. Sector-wise examination revealed that the nighttime lights had the highest coefficients for the GDP of secondary or the manufacturing sector [10]. In another study, relationship between nighttime lights and households within different income brackets at the district level for India was examined. It was observed that although a good relationship exists between nighttime lights and households in low, middle, and high income brackets, the relationship is much stronger for households in higher income brackets than those in the lower income brackets [11].

Mellander *et al.* [17] investigated the relationship between stable lights and radiance-calibrated nighttime lights, and economic activity, population, and establishment density, for geo-coded micro-data of Swedish establishments and individuals. They found that the nighttime lights could serve as a better proxy for population and establishment density, indicating levels of urbanization rather than total population. They also suggested the nighttime lights were a good indicator or proxy measure of number of establishments, or total production and consumption in terms of wages. They also found that the radiance-calibrated images had a stronger correlation with economic activity than the stable lights images.

## 2.2. Nighttime Lights and Poverty

Poverty is antithetical to human well-being. Therefore, attempts are made to quantify areas of poverty and population in poverty so that aid and development resources can be targeted most effectively and efficiently. Consequently, poverty maps assume great importance. However, many poverty maps are available only at the national level in which one value is representative of an entire administrative unit. Elvidge *et al.* [18] conducted a novel study by creating the first spatially disaggregated 1 km<sup>2</sup> resolution map of population in poverty. Two spatially disaggregated data sources—the nighttime stable lights satellite image of 2003 along with the LandScan population grid of 2004 were used for this purpose. The LandScan 2004 grid depicting population count numbers were divided by the average visible band digital number from the stable lights nighttime image to develop the grid of Poverty Index (PI). In areas where population was present but no light was detected, the full population count was passed to the index (Equation (7)).

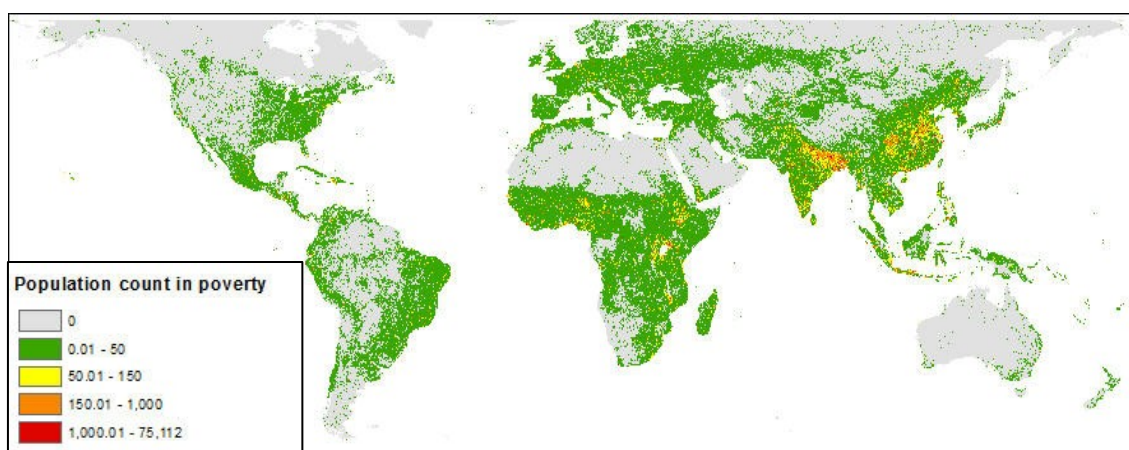
For estimating the population in poverty, a calibration was developed based on the poverty line data available from the World Development Indicators (WDI) 2006 national level estimates. The international poverty line in WDI in purchasing power parity was specified in terms of the number of individuals living on less than \$1.08 and \$2.15 a day at 1993 international prices. The calibration was developed on the basis of the WDI 2006 national level estimates for the percentage of people living on \$2 or less per day [41]. To establish the calibration, the sum of the PI values was extracted for each country, divided by the total population count, and then multiplied by 100 to form a Normalized Poverty Index (NPI). The NPI was then regressed to the percentage of population living on \$2 per day or less and this gave an R<sup>2</sup> of 0.72 (Equation (8)).

$$\text{Poverty Index (PI) at the grid level} = \frac{\text{LandScan 2004 population grid}}{\text{Stable lights nighttime image of 2003}} \quad (7)$$

$$\text{Normalized Poverty Index (NPI) at the country level} = \frac{\text{Sum of PI for each country} \times 100}{\text{Total population of each country}} \quad (8)$$

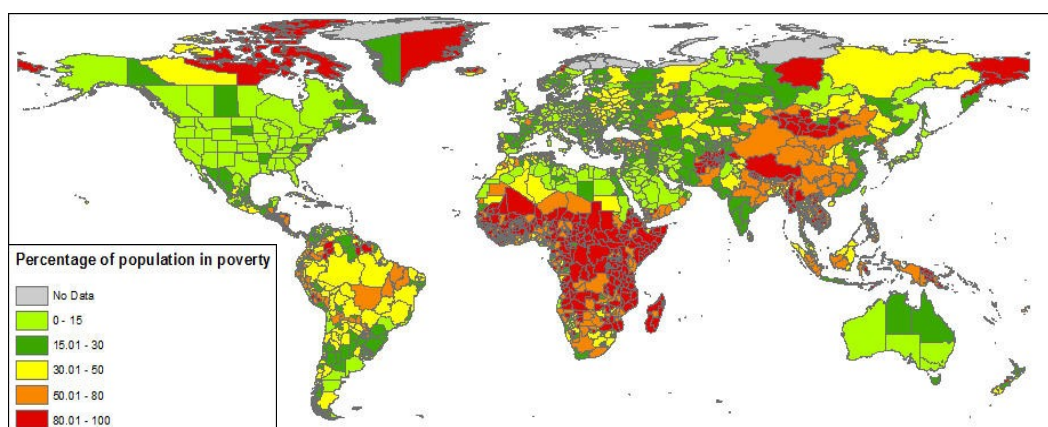
The calibration coefficients derived from the regression were applied to the NPI grid to get a percent estimate of poverty in each grid cell and then multiplied with the population count grid to yield an estimate of the population count in poverty (poverty count) (Figure 4).

**Figure 4.** Poverty count grid.



Poverty count could then be aggregated to the national or sub-national level. Aggregating the poverty counts to the sub-national level administrative units (states/provinces) (Figure 5) gave rise to patterns which matched expected patterns, with lower poverty levels in the more prosperous areas. For instance, coastal China showed lower poverty levels than interior areas, north-eastern India showed higher poverty rates than western and southern India, and the prosperous Sao Paulo region of Brazil demonstrated as having lower poverty rates than the rest of Brazil.

**Figure 5.** Percentage of population in poverty for sub-national administrative units based on satellite data-derived poverty index.



Nighttime light images were used as a proxy measure of poverty at the Administrative 1 level for African countries to enable health interventions in the most required areas [19]. Mean brightness of nightlight pixels, distance to nightlight pixels, and proportion of area covered by nightlights were computed for each administrative level polygon. Asset-based indices were computed from national household survey data using principal components analysis. Correlation was examined between the asset-based indices and the three nightlight metrics in both continuous and ordinal forms. It was seen that the mean brightness of nightlights had the highest correlation coefficient with the asset-based wealth index in both continuous and ordinal forms. Realizing the usefulness of these nightlight metrics as a proxy for asset-based indices, the authors concluded that this proxy variable could be used to explore economic inequality in health outcomes and access to healthcare facilities at sub-national level, when data at the required resolution are not available.

Understanding the importance of estimating regional poverty levels for undertaking measures for eradicating poverty, Weng *et al.* [20] investigated the value of the DMSP-OLS stable lights nighttime imagery in estimating regional poverty for 31 regions at a provincial scale for China. Principal component analysis (PCA) was used to develop an integrated poverty index (IPI) from 17 socio-economic indexes, which have been proven to be good representatives of poverty levels in China. Average Light Index (ALI) was computed for each region on the basis of the total number of lit pixels. Regression analysis between IPI and ALI for the 31 provinces in China gave an  $R^2$  of 0.85. This research proved yet again the significance of the nighttime images as a proxy variable in analyzing poverty at the regional level.

Perhaps the most recent and important recognition of using nighttime lights as a proxy variable for estimating poverty came up in the DC Big Data Exploration workshop held between 15–17 March 2013 in Washington, DC, USA. DataKind, in partnership with the World Bank, and its partners UNDP, UNDB, UN Global Pulse, and the Qatar Computing Research Initiative, conducted the workshop to explore innovative ways to fight poverty and corruption [21]. A team of experts in the span of a weekend explored the possibility of the nighttime image to be used as a substitute variable for estimating sub-national poverty levels. They overlaid light information with other geospatial indicators (for example, population, change in poverty) and performed statistical analysis illustrating that lighting levels in the nighttime images could predict poverty level in 2001 for Bangladesh. They put forward their suggestion to the World Bank to use these findings to carry out more sophisticated experiments relating nighttime lights and poverty, and to construct a software application which would enable monitoring poverty in real-time from remote sensing images.

### *2.3. Use of Nighttime Lights for Estimating Informal Economic Activity and Remittances*

One of the criticisms of GDP as a measure of social welfare is that it does not take into account the informal transactions in the economy. For example, transactions of street vendors in Mexico City, rickshaw pullers in Kolkata, barbers, cobblers, and vendors selling a diverse array of products including vegetables, fruit, cigarettes, toys, *etc.*; women selling goods or produce from their homes, garment makers, embroiderers, are all informal workers, whose transactions are not recorded in the national accounts. However, informal economic activities are a means of livelihood for large fractions

of populations, especially in developing countries. Informal economic activity is essential to many people's very survival.

Remittances are the funds that the international migrants send back to their countries of origin. Remittances contribute to the Gross National Income (GNI) of a country, where GNI is the sum of GDP plus net receipts of compensation of employees and property income from abroad. Remittances are a major source of external financing in developing countries and often help to improve the economic conditions of families in domestic countries. Obtaining official estimates of inflow of remittances is fraught with problems.

Because of the problems associated in obtaining informal economy estimates, an attempt was made by Ghosh *et al.* [23] to estimate informal economy using nighttime light image. This was based on the assumption that since the official estimates of GSP, GDP, and GNI, are believed to include most of the formal transactions in the economy, any surplus of these economic values measured from the spatial patterns of nighttime lights can be attributed to informal economy and inflow of remittances, which often are underestimated in the official figures. Thus, models were developed to estimate the Gross Domestic Income, informal economy and remittances of Mexico on the basis of the spatial patterns of nighttime lights and the more reliable official figures of Gross State Product (GSP) of the United States (U.S.). The radiance-calibrated nighttime satellite imagery data of 2000–2001, and the LandScan population data of 2000 were used in this study.

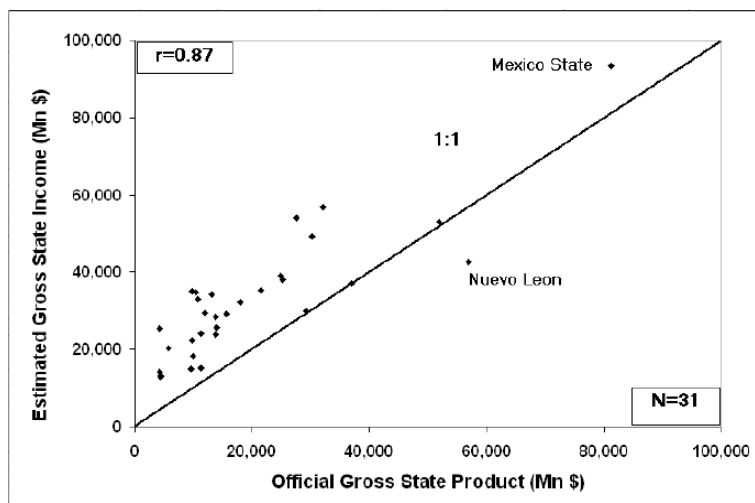
In the model developed, a brightness threshold was selected to determine the lit urban regions of the U.S. on the DMSP-OLS nighttime image. Aggregated values of the lit areas were obtained for all the U.S. states. Population sums of the corresponding lit areas were acquired from the LandScan population grid. Then on the basis of the law of allometric growth [42], and the aggregated values of the areas and populations of the U.S. states, estimated populations of the U.S. states were computed. Next, a multiple regression model was developed to estimate the Gross State Income (formal plus informal economy) for each U.S. state, using the estimated urban population of each state, the sum of light intensity value of all lights above zero for each U.S. state, and GSP of each U.S. state inflated by adding 10 percent of informal economy contribution to the GSP of each state [43,44]. In the next step, the same threshold which was used to demarcate the urban areas of the U.S. was used to demarcate the urban regions of Mexico, and the “U.S. equivalent” urban population of Mexico was estimated ( $P'_{\text{Mexi}}$ ) using the model developed for the U.S. The same regression model developed for the U.S. was used to estimate the Gross State Income ( $\text{EGSI}_{\text{Mexi}}$ ) of each Mexican state using the “sum of lights” for each Mexican state ( $S_{\text{Mexi}}$ ) and estimated urban population of each Mexican state ( $P'_{\text{Mexi}}$ ) (Equation (9)).

$$\text{EGSI}_{\text{Mexi}} = \alpha_{\text{USi}} + \beta_{\text{USi}} \times P'_{\text{Mexi}} + \beta_{\text{USi}} \times S_{\text{Mexi}} \quad (9)$$

The  $\text{EGSI}_{\text{Mexi}}$  was assumed to include the formal economy, informal economy, and inflow of remittances. Adding the EGSI of each Mexican state provided the Estimated Gross Domestic Income ( $\text{EGDI}_{\text{Mex}}$ ) for Mexico. The EGSI values were compared to the GSP values of each Mexican state, although they should be compared with the GNI values. However, GNI values were not available at the state level. Plotting the EGSI of Mexico against the GSP of each Mexican state, excluding Distrito Federal or Mexico City, showed that GSP of Mexico was overestimated for 27 Mexican states and

underestimated for one state. The Pearson's correlation coefficient of the official GSP *versus* modeled EGSI was 0.87 indicating a strong association between the two variables (Figure 6).

**Figure 6.** Official GSPMexi *versus* Modeled EGSI Mexi of the Mexican states, excluding Distrito Federal. (Source: adapted from [23]).



The model underestimated the EGSI of Mexico City by 86 percent in comparison to the official GSP. Thus, the EGSI of Mexico City was an outlier, and had to be excluded from the graph. However, it was included in the calculation of the  $EGDI_{Mex}$ . In the last step of the analysis, underestimation of informal economy (UIER) and remittances in the official GNI estimate was calculated by subtracting the GNI of Mexico from the  $EGDI_{Mex}$ . The result demonstrated that the informal economy and inflow of remittances for Mexico was about 150 percent larger than what was recorded in the official estimates of Gross National Income (GNI) (Table 1).

**Table 1.** Determining the magnitude of underestimation of informal economy and remittances in the official estimates of GNI of Mexico. (Source: adapted from [23]).

Row No.		In U.S. \$ billions
1	Nighttime lights Estimated GDI of Mexico ( $EGDI_{Mex}$ ) (formal+informal+remittances)	1,041
2	Official estimates of the GNI of Mexico ( $GNI_{Mex}$ ) (formal+informal+remittances) *	886
3	Predicted underestimation of remittances and informal economy (UIER)	155
4	Official estimates of Informal economy in 2000 *	99
5	Official estimates of remittances in 2000 ♦	7
6	Total official estimates of informal economy and remittances	106
7	Predicted underestimation of remittances and informal economy	155
8	Total official estimates of informal economy and remittances	106
9	Magnitude of underestimation	~ 150%

\* Data source: INEGI, Sistema de Cuentas Nacionales de Mexico, Producto interno bruto, a precios de Mercado, 1999-2004; ♦ Source: INEGI, *Sistema de Cuentas Nacionales de México, Cuentas por Sectores Insitucionales, Cuenta Satelite del Subsector informal de los hogares*, 1998-2003;

♦ Data source: Bank of Mexico, Annual Report, 2004.

The model provided an objective and independent measure of economic activity based on the spatial pattern of lights and the more reliable measure of economic activity of a developed country. Even with its flaws it can be looked upon as an approach, which provides a standardized methodology for estimating economic activities, including informal economy and remittances, for all countries of the world, as well as the potential for estimating disaggregate economic activity at the sub-national level.

#### *2.4. Use of Nighttime Lights for Developing the Night Light Development Index (NLDI)*

There is an increasing recognition that the distribution of wealth and income amongst the population in a nation or region correlates strongly with the level of human development of the population of that nation or region. This in turn is correlated to the happiness and well-being of the population of the nation or region [45]. Gini coefficients derived from Lorenz curves are a well-established method for measuring income distribution. However, measuring the distribution of wealth and income at national and regional scales is a challenging problem. Thus, an alternative measure of the distribution of wealth was developed using the nighttime lights image and the LandScan population grid. This was called the Night Light Development Index (NLDI) [24].

The NLDI was developed using the same concept of the Lorenz curve and Gini coefficient. A tabular list was created with data on population count extracted from the LandScan population grid of 2006, and lighting radiance data extracted from the radiance-calibrated nighttime image of 2006. The tabular list was sorted from the dimmest to the brightest, and the cumulative percentages of light and population were calculated. The Lorenz curve was drawn after plotting the cumulative percentage of population on the x-axis and the cumulative percentage of light on the y-axis. The ratio of the area between the diagonal line of 45 degrees (depicting the line of perfect equality) and the Lorenz curve (pink area in Figure), and the area between the line of perfect equality and perfect inequality (yellow area in Figure) gave the NLDI (similar to the Gini coefficient). The NLDI varies from 0 to 1 as does the traditional Gini Coefficient and the Human Development Index (HDI) (Figure 7).

The NLDI measures how emitted light as observed by the DMSP-OLS is spatially distributed relative to the spatial distribution of the human population. If one person in a nation or region had lived by themselves in the only square kilometer that produced nighttime light emissions detected by the DMSP-OLS then that nation or region would have a spatial Gini coefficient of 1.0. If all people in a nation or region lived in areas of the country such that they all had the same average amount of nighttime light emission per person the NLDI would have a value of 0.

NLDI coefficients were calculated at the global level, national level (for each country), at the sub-national level (for each state or province within each country), and at the Gridded level (that is on a quarter degree grid, with no consideration of national or sub-national boundaries). The global NLDI was 0.893 and was driven to higher values by the 1.2 billion people who live in areas with no detectable lighting. The NLDI values at the national level depicted a wide range of values with the overall trend being such that highly developed countries had low NLDI values, and less and least developed countries had high values. Island states were also seen to have unusually low NLDI values.

NLDI values for the sub-national units (primarily states and provinces) made it possible to see the variation of NLDI within individual countries (Figure 8). It was observed that developed, urbanized, and industrialized areas within countries have higher sub-national NLDI values than the less developed

areas. For instance, eastern China, which is more developed than the western Chinese provinces, had much lower NLDI values. Again, for India, the developed areas around Bangalore, Hyderabad, Mumbai and Delhi had lower NLDI values than the rural interior areas between Delhi and Kolkata. The gridded NLDI at a spatial resolution of 0.25 degree provides great spatial detail revealing the variation in the NLDI values within countries on a uniform spatial grid (Figure 9).

Figure 7. Graphical representation of the Gini coefficient. (Source: adapted from [24]).

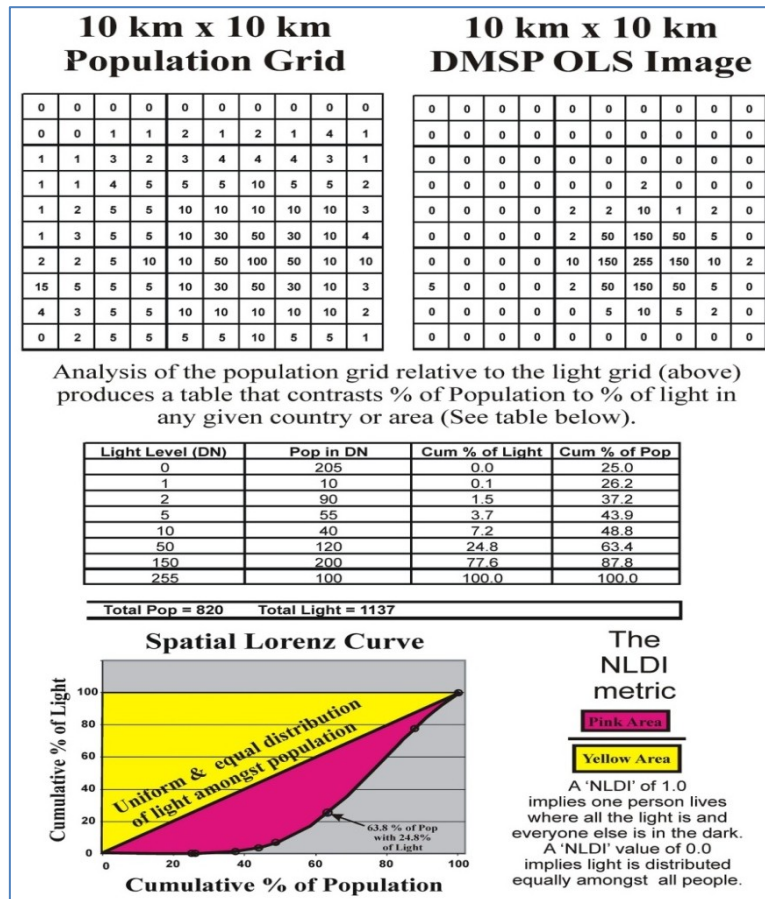


Figure 8. Map of sub-national Night Light Development Index (NLDI) values.

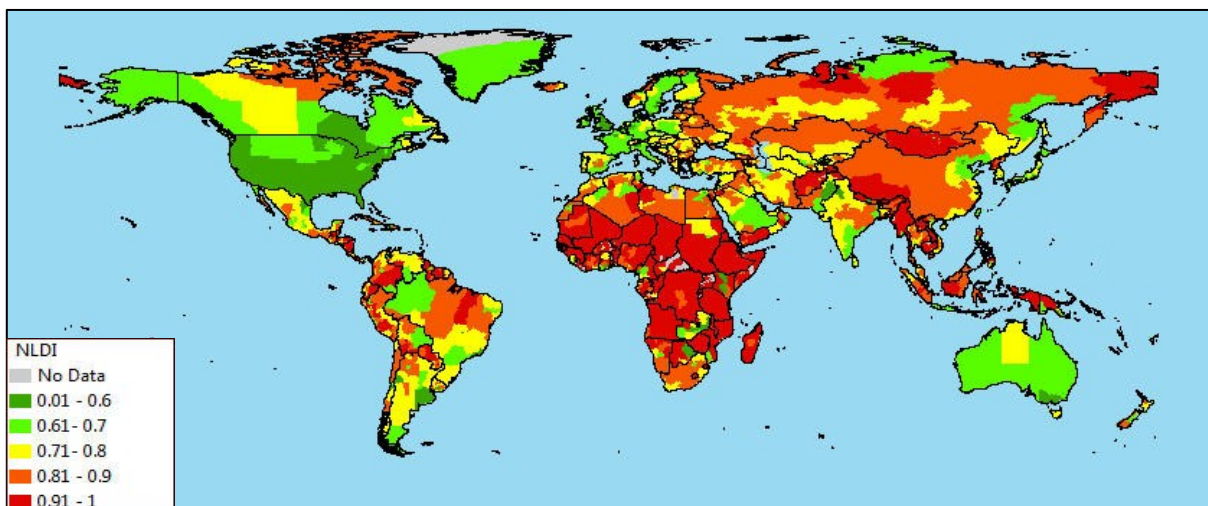
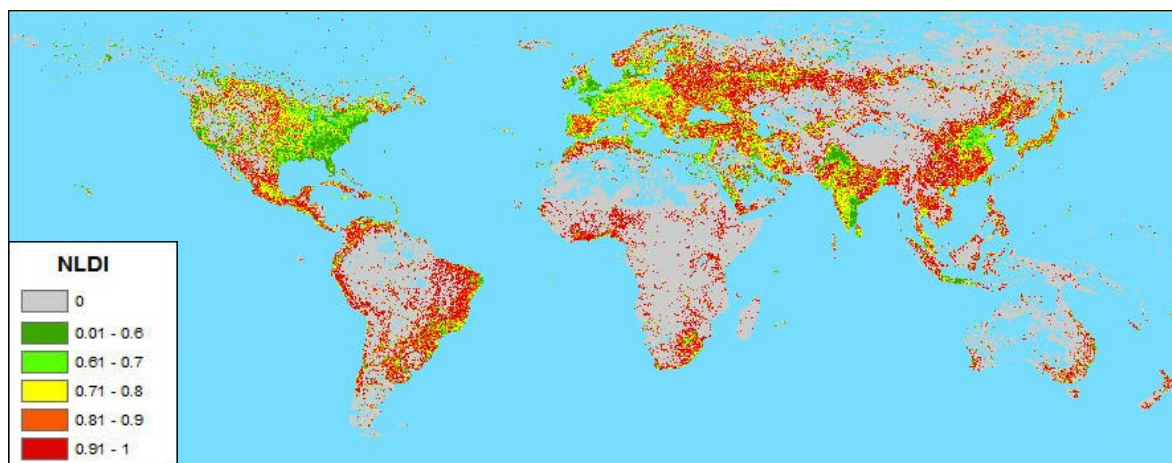
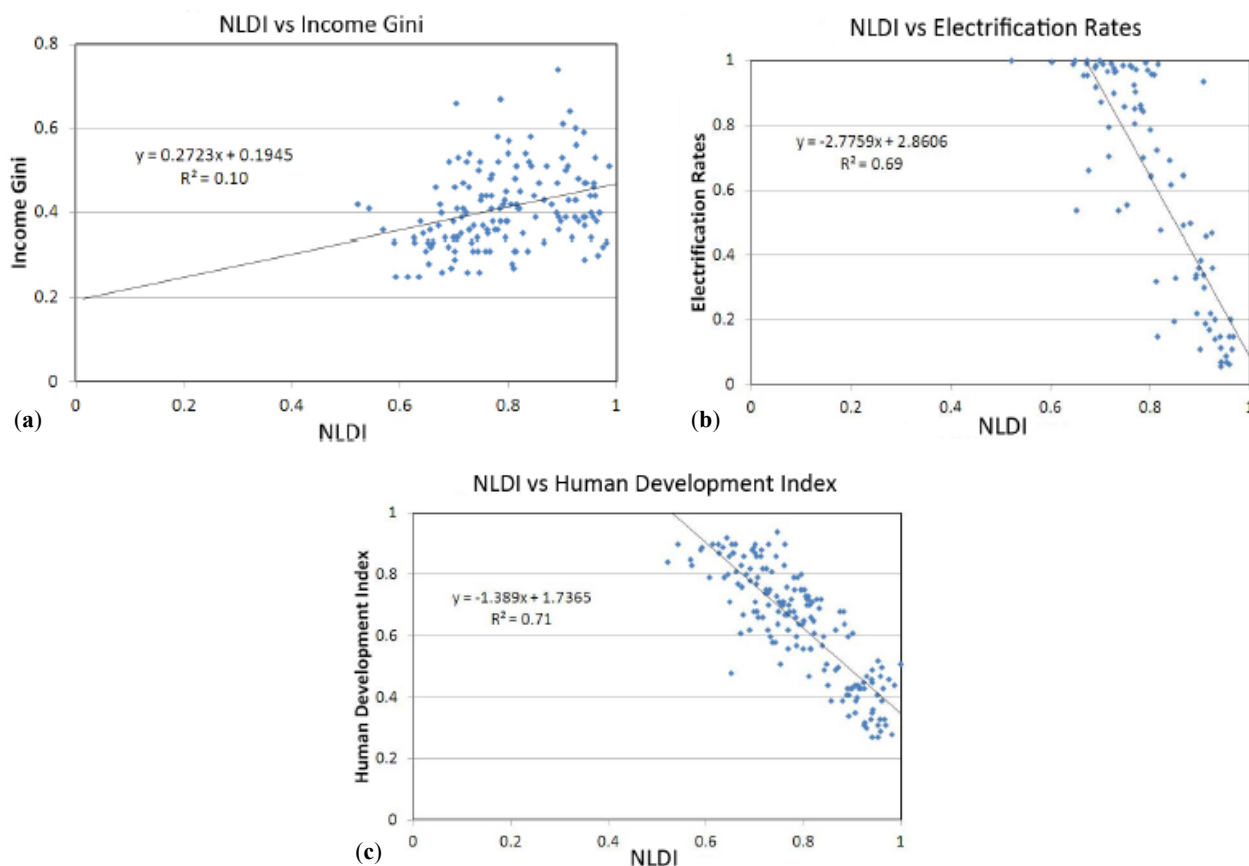


Figure 9. Spatial grid of NLDI values.



Correlations were examined between the country-level NLDI and several other national level indices, including the income Gini coefficient. The NLDI showed weak correlations with traditional Gini coefficients measured by the World Bank with an  $R^2$  of 0.1 (Figure 10a). However, the NLDI showed strong negative correlations with the electrification rates (Figure 10b) and Human Development Index (HDI) (Figure 10c) with  $R^2$  values of 0.69 and 0.71, respectively.

Figure 10. National NLDI vs. Income Gini, Electrification rates, and Human Development Index. (Source: adapted from [24]).



The weak relationship between NLDI and the income Gini highlights the fact that brightly lit areas in the DMSP imagery correspond to areas of high population densities having a varied mix of individual income levels and not only to lower population densities of a few wealthy people. Thus, even though the Lorenz curve methodology of measuring income inequality motivated this work, it was realized that NLDI was a more appropriate index for measuring development than income distribution. The HDI is a composite statistic that uses life expectancy, literacy, education, and standards of living to measure human well-being. The strong inverse relationship between NLDI and HDI influences the consideration of NLDI as a supplemental measure of human development.

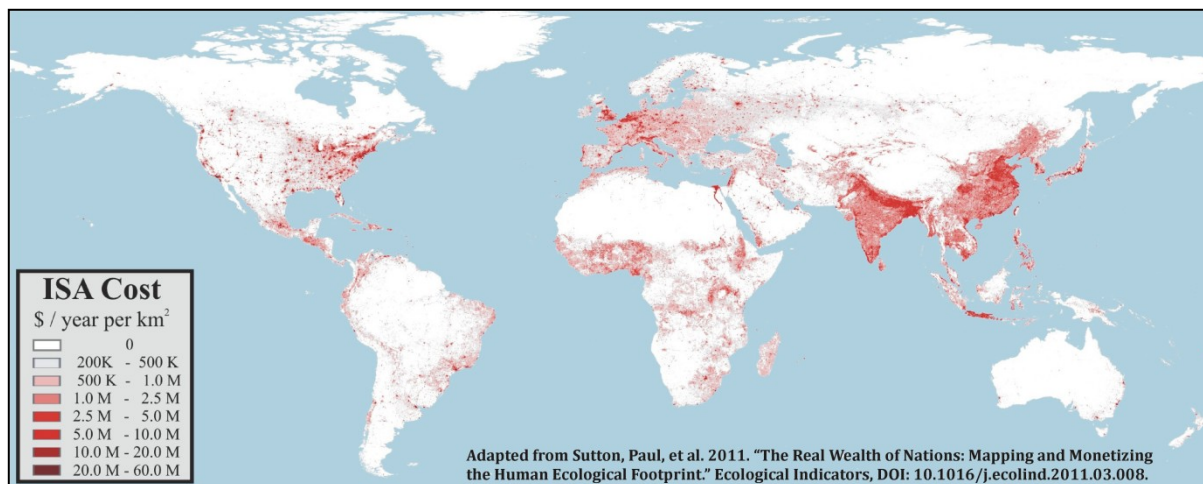
### *2.5. Use of Nighttime Satellite for Mapping and Monetizing the Human Ecological Footprint*

Since the nighttime light images correspond to areas of human habitation, the anthropological impacts of human activities were also studied using these images. Minimizing the human ecological footprint and not exceeding the carrying capacity of the earth have become key ecological indicators of the bio-physical sustainability for the human race. Human well-being is undoubtedly linked to leading a sustainable lifestyle.

A new method was devised for measuring anthropogenic environmental impact, which was monetized as an environmental cost. Two global maps—Net Primary Productivity (NPP) and Impervious Surface Area (ISA) were used for this purpose. Anthropogenic Impervious Surface Area (ISA) was used as a spatially explicit proxy measure of human “demand” on the planet and NPP was used as a spatially explicit proxy of the ecosystem services “supplied” by the planet. ISA are those land surfaces that have been converted by human action to impervious surfaces. These two global values were set to the same number (\$50 trillion), with the assumption that the human impact on the world is balanced by the earth’s ability to absorb the impact. This assumption causes the resulting table of national deficits and national surpluses to have a zero sum. The final map presented a map of ecological surpluses and deficits (in U.S. dollars). This map was summarized at the country level for easy comparisons.

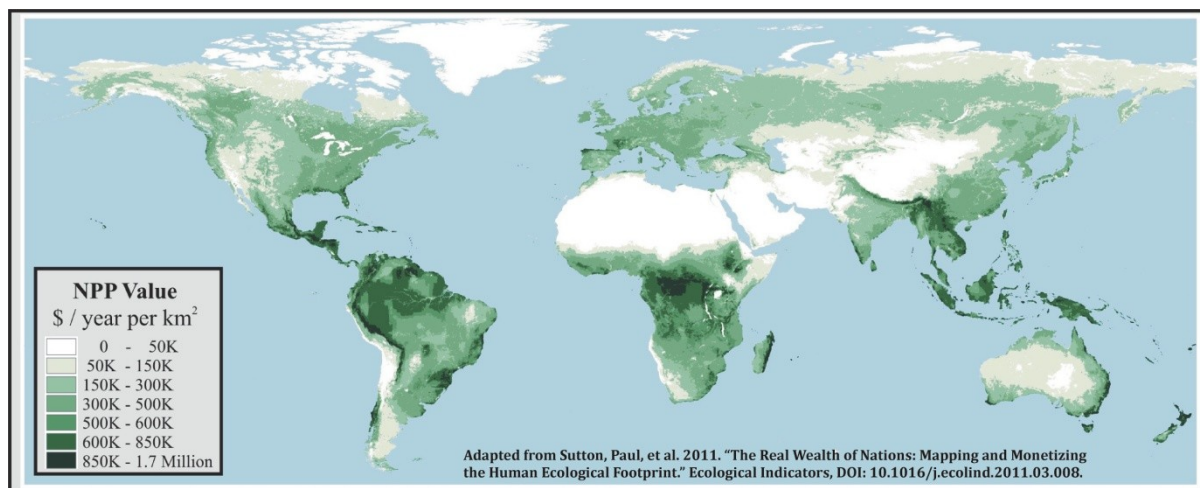
The ISA map was made from the nighttime satellite imagery, LandScan population data, and impervious surface area data for the conterminous USA derived from Landsat. High-resolution aerial photography was used to develop regression parameters to create a model for predicting impervious surface area with nighttime lights and population. The U.S. Geological Survey (USGS) impervious surface product for the conterminous USA was used as calibration data for the model. The final product was a 1-km<sup>2</sup> resolution grid with a global distribution of 580,000 km<sup>2</sup> of impervious surface area. The ISA per person and Ecological footprint (developed by Wackernagel and Rees, [46]) in global hectares (gha) per person were shown to be highly correlated with an  $R^2$  of 0.78. The pixel values of the ISA product ranged from 0 to 100 percent [47]. The \$50 trillion dollars was disaggregated to those pixel values on a simple linear basis to produce the monetized map of human impact on earth (Figure 11).

**Figure 11.** Anthropogenic impervious surface area monetized to \$50 Trillion for the year 2000.



In an identical manner, \$50 trillion dollars were disaggregated to a global dataset of NPP developed and disseminated at the Oak Ridge National Laboratory [48]. NPP is the “*net amount of solar energy converted to plant organic matter through photosynthesis. It can be measured in units of elemental carbon and represents the primary food energy source for the world’s ecosystems*”. In the model developed, the dollar values of earth’s renewable natural endowment was produced by spreading \$50 trillion dollars in a simple linear allocation to the pixel values of this global NPP dataset (Figure 12).

**Figure 12.** Net primary productivity monetized to \$50 Trillion for the year 2000.



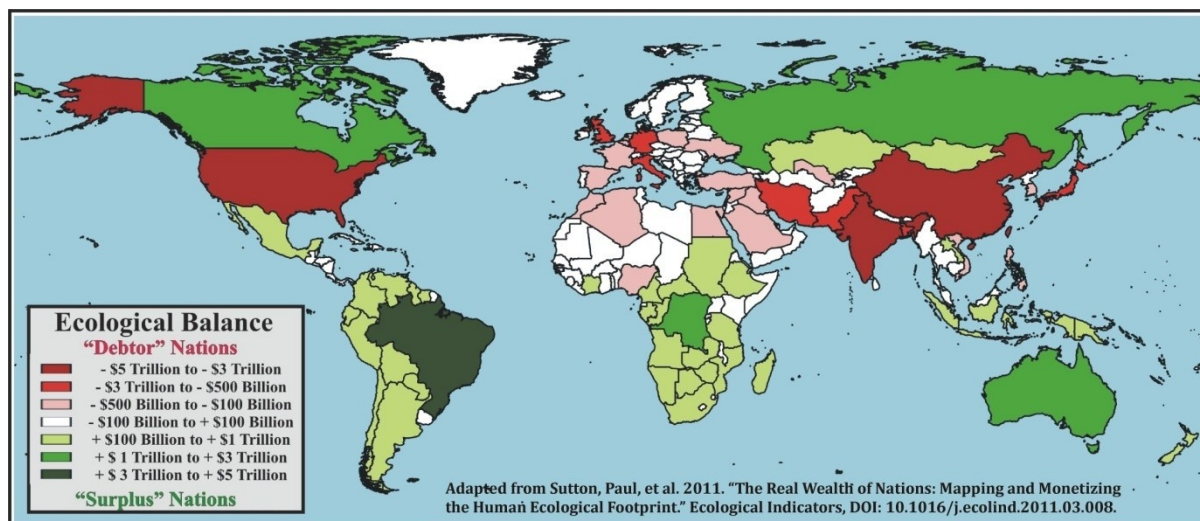
The monetized ISA and NPP images were converted to be in the same resolution ( $1 \text{ km}^2$ ) and same projection (Mollweide equal area projection). Then these two images were subtracted to create a global map of the surplus or deficit value of natural production (NPP)–Human Impact (ISA). The assumption was that humanity was presently at or about carrying capacity (Equation (10)).

$$\text{NPP (monetized to \$50 trillion)} - \text{ISA (monetized to \$50 trillion)} = \text{Ecological balance} \quad (10)$$

(i.e., Natural production “supply” – Human Impact “demand” = National Surplus or Deficit).

The resulting grid of ecological balance was aggregated to national or country levels of aggregation (Figure 13). For each country, the total value of NPP (\$NPP), Total Cost of ISA (\$ISA), the difference between \$NPP and \$ISA (Eco-balance), and Eco-balance per capita were calculated.

**Figure 13.** Map of country level ecological balance.



The regions of highest surplus values were found in Russia, Brazil, Australia, Canada, Central Africa, Central America, and parts of Southeast Asia. These regions are operating their national economies below the carrying capacity of their national ecosystems. These patterns correspond with another study that used the value of the nation’s ecosystem services instead of NPP and nighttime satellite imagery instead of ISA [49]. However, many of these areas are losing vital ecosystem services because of rapid deforestation. On the other hand, regions such as North America, China, India, and Europe, show ecological deficits, which implies that high levels of human development and population are exceeding natural production values. In these regions national production and consumption levels have exceeded ecological capacity.

The ecological balances measured for the countries were found to have a high correlation with Ecological Deficit metrics established up by the Global Footprint Network [49]. Because of the large amount of data required to generate Ecological Deficit numbers, and since data are not available for some countries, the simple metrics available from this method of ecological accounting serve as a useful supplement to Ecological Deficit Data.

## 2.6. Nighttime Lights and Electrification Rates

Access to electricity is also considered to be an indicator of quality of life. Having limited or no access to electricity gives rise to conditions which are unfavorable to human health and well-being, such as lack of refrigeration for food, poor water and sanitary facilities, limited access to health care services. For many people the absence of electricity brings life to a standstill after sunset.

The DMSP-OLS nighttime lights imagery in combination with the LandScan population grid have been used to measure electrification rates as an indicator of quality of life [26]. Both the stable lights nighttime imagery and the LandScan population grid were for the year 2006 (Figures 14 and 15).

**Figure 14.** Color composite image made with the 2006 LandScan population grid and the 2006 Defense Meteorological Satellite Program (DMSP) nighttime lights. In the developed world there is an abundance of lighting yielding a cyan color. Red areas indicate dense population with no detectable DMSP lighting.

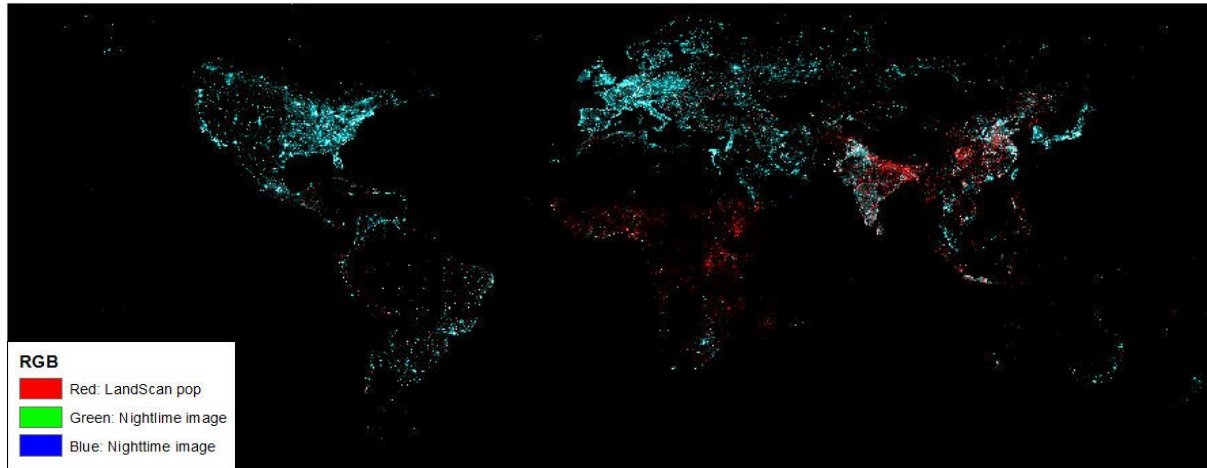
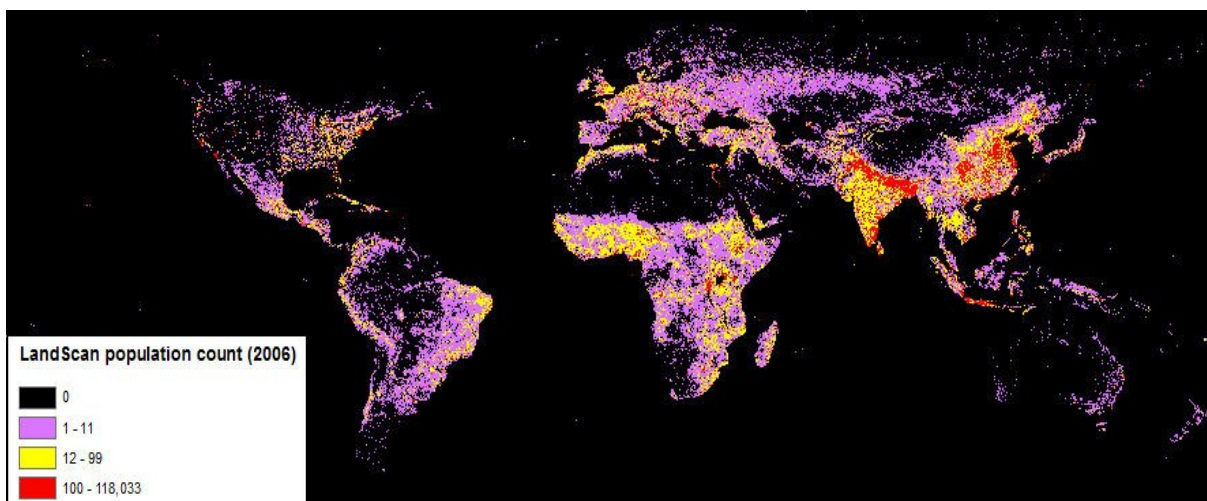


**Figure 15.** LandScan population count per grid cell, 2006.



The national level reference data on the extent of electrification were taken from the International Energy Agency's (IEA) World Energy Outlook (WEO), 2006 [50–52]. The IEA has admitted to having no internationally accepted definition for electric power access and no standardized method for data collection. This is yet another example of how the use of two gridded data products derived from censuses, satellite imagery, and spatial analysis can provide useful and valid proxy measures.

From the nighttime imagery, lighting from the gas flares was masked out. The locations of gas flares in the DMSP nighttime lights had been demarcated using high-resolution imagery in Google Earth in a study done earlier [53]. The remaining lights in the DMSP imagery are necessarily from electric lighting. A binary mask was created for areas lit by gas flares. This mask was applied on the LandScan population grid to zero out the population in areas lit by gas flares. A second mask was created for the remaining lights. This mask was used to divide the gas-flare-free population into two segments: (A) population with lighting detected (Figure 16); (B) population with no lighting detected (Figure 17).

**Figure 16.** LandScan population count in areas with DMSP detected lighting.

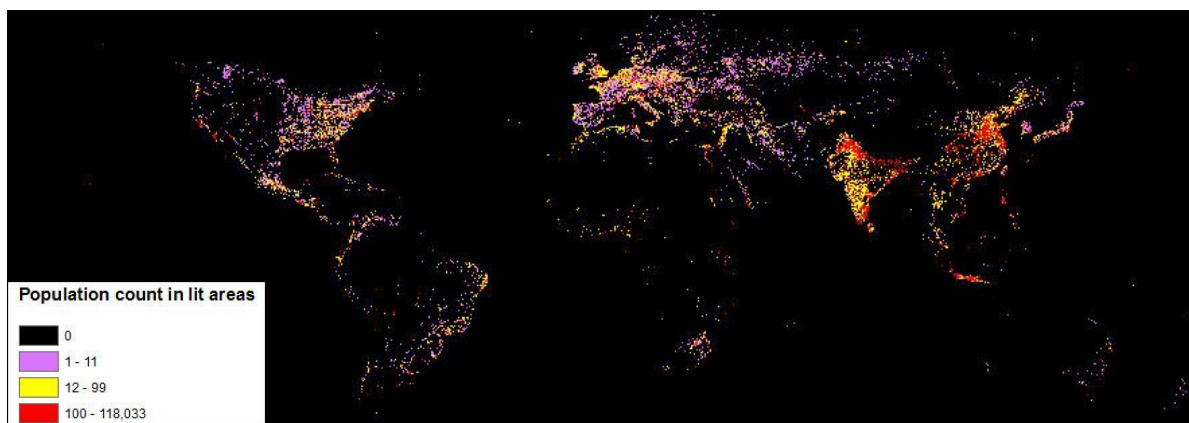
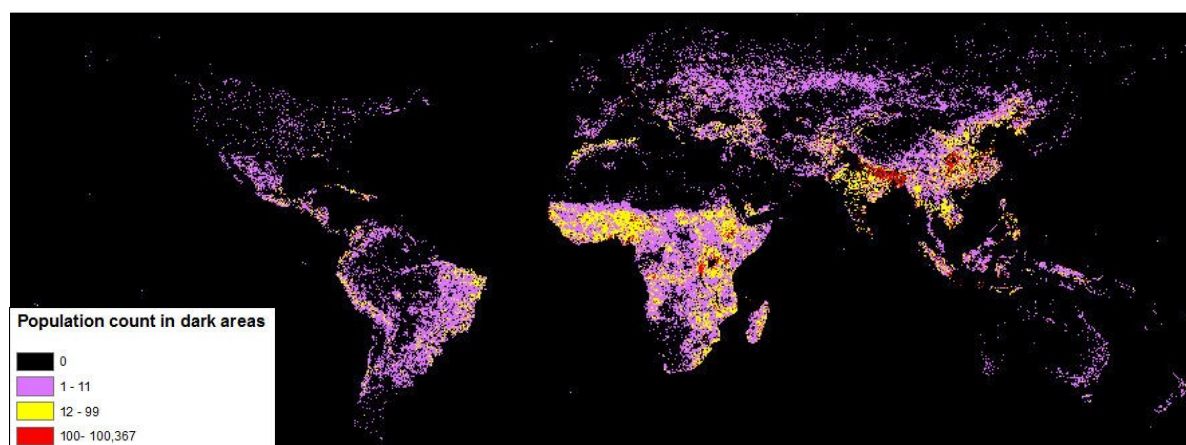


**Figure 17.** LandScan population count in areas with no DMSP detected lighting.



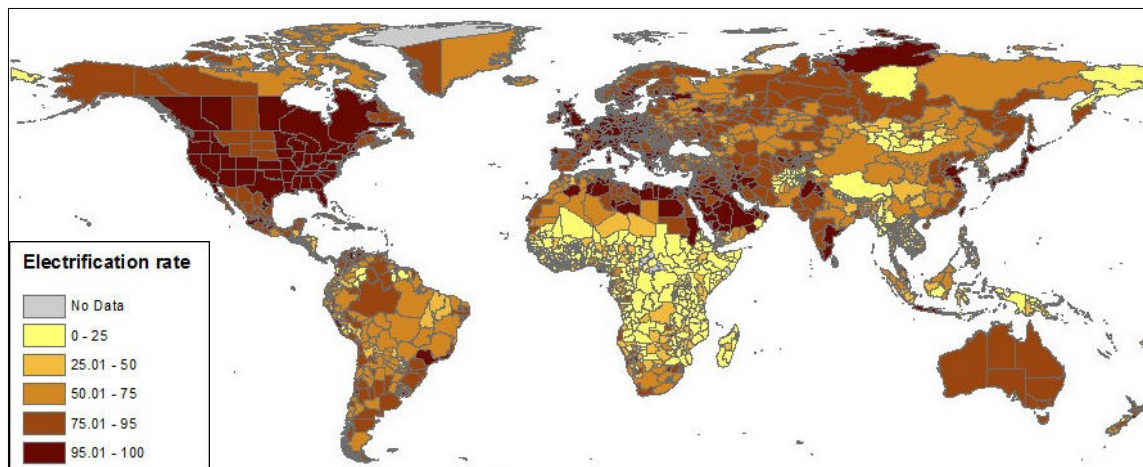
The percent electrification rate was then calculated as (Equation (11)):

$$\frac{\text{Population with DMSP lighting (A)}}{\text{Total Population (A + B)}} \times 100 \quad (11)$$

Since the LandScan data is a disaggregated map it could be aggregated to national, sub-national or any user-defined spatial aggregations. The aggregation was done at the national and the sub-national (states and provinces) level (Figure 18). The total number of people found to be without electricity was 1.62 billion, only about 2.5 percent larger than the 1.58 billion estimated by the IEA. The electrification rates for the countries as estimated from the DMSP nighttime lights were in an overall agreement with the IEA electrification rates. Developed countries for which IEA reported near 100 percent electrification rates, yielded DMSP estimated electrification rates ranging from 98 to 100 percent. The countries for which the DMSP estimated electrification rates were less than 20 percent are some of the poorest countries in the world.

However, there were cases where they differed substantially. Among the top 10 countries where the IEA reported electrification rates were higher than the DMSP estimates were Thailand, China, and Cuba with more than 20 percent difference between the two numbers. Countries reported by the IEA as having 10–20 percent higher electrification rates were Brazil, Paraguay, Mongolia, Cameroon, and Algeria.

**Figure 18.** DMSP estimated electrification rates for sub-national units (states and provinces) for the year 2006.



Among the countries for which the DMSP estimated electrification rates were higher than the IEA estimates were Iraq, Congo, Pakistan, Sri Lanka, Qatar, Indonesia, Lesotho, Bangladesh, Afghanistan, Gabon, and India. For both India and China it was noticed that the core of the DMSP identified population with no detected lighting were located in the heavily populated and the poorest zones of the nations (Figure 18).

Even though this method of estimating electrification rates is not flawless, the nighttime lights and population grid produced the first global systematic global assessment of electrification rates as an indicator of human well-being.

Chand *et al.* [54] studied the socio-economic development of Indian states and cities over a decade (1993 to 2002) by looking into the spatial and temporal changes in electric power consumption using the nighttime lights data obtained from the DMSP-OLS images over the Indian region. Information of changes in light situation over the decade was integrated with demographic and electricity consumption data for India, and it was seen that an increase in population over the decade was accompanied by a simultaneous increase in power consumption and an overall increase of about 26 percent nighttime lighting. Correlation analysis between increase in population to the increase in nighttime lights and electric power consumption gave  $R^2$  values of 0.59 and 0.56, respectively. Moreover, an increase in light intensities along the peripheries of major Indian cities was observed. Some states, however, showed a decline in nighttime lights, which could be primarily attributed to declined economic growth and poverty in those states.

### 2.7. Use of Nighttime Satellite Imagery for Estimating the Information and Technology Development Index (IDI)

The development of societies as information societies is another measure of the progress and well-being of societies. The International Telecommunication Union (ITU), a United Nations Agency, has developed a tool known as the Information and Communication Technology Development Index (IDI) to measure the development of countries as information societies. The IDI is a composite index made up of 11 indicators covering Information and Communication Technology (ICT) use, access, and

skills. Most of the indicators included in the IDI were found to have a close relationship with GDP per capita [55]. This encouraged the possible investigation of using nighttime lights as a proxy measure of IDI through its utilization in creating the GDP grid [8].

The use of the nighttime lights imagery in creating the GDP grid has already been discussed in the previous section. The disaggregated map of total economic activity was aggregated to the country level for all countries of the world. The aggregated GDP values were then divided by the population of the countries to get GDP per capita values. A second-degree polynomial regression relationship was established between the estimated GDP per capita and the official IDI values. This regression relationship gave an  $R^2$  of 0.89 and provided estimated IDI values for all countries of the world (Figure 19). Plotting the official *versus* estimated IDI for all countries of the world with a 1:1 line showed that the estimated IDI has a strong association with the official IDI with a Pearson’s correlation coefficient (R) of 0.97 (Figure 20).

**Figure 19.** Second-degree polynomial regression for estimating Information and Communication Technology Development Index (IDI). (Source: adapted from [27]).

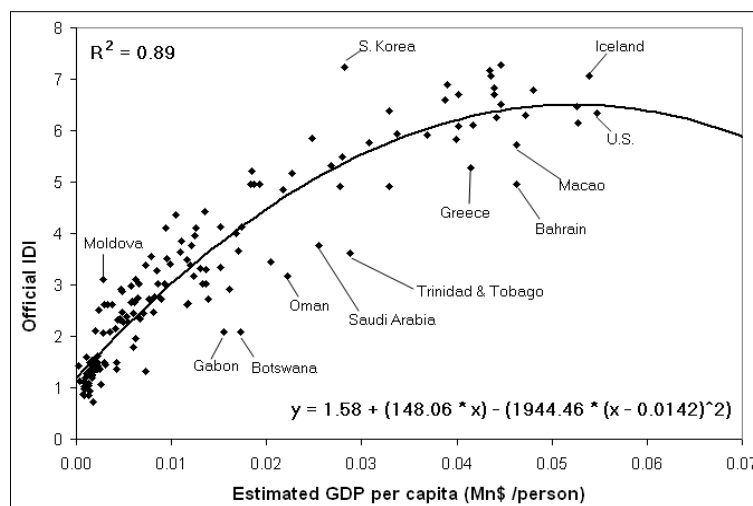
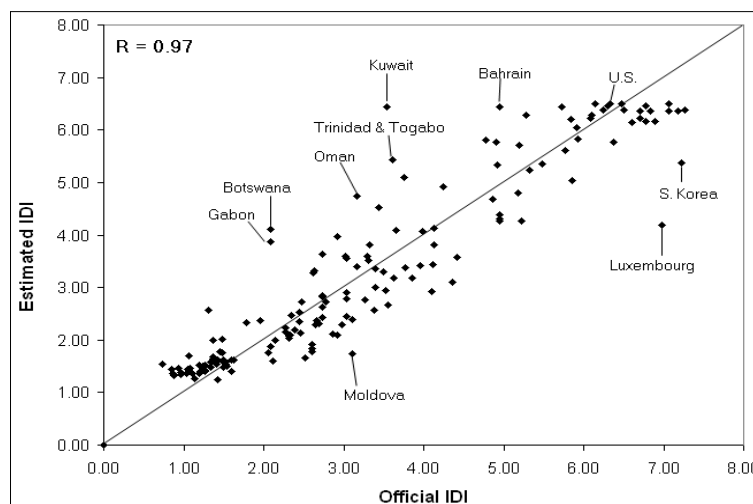


**Figure 20.** Official IDI *versus* Estimated IDI for the countries of the world. (Source: adapted from [27]).

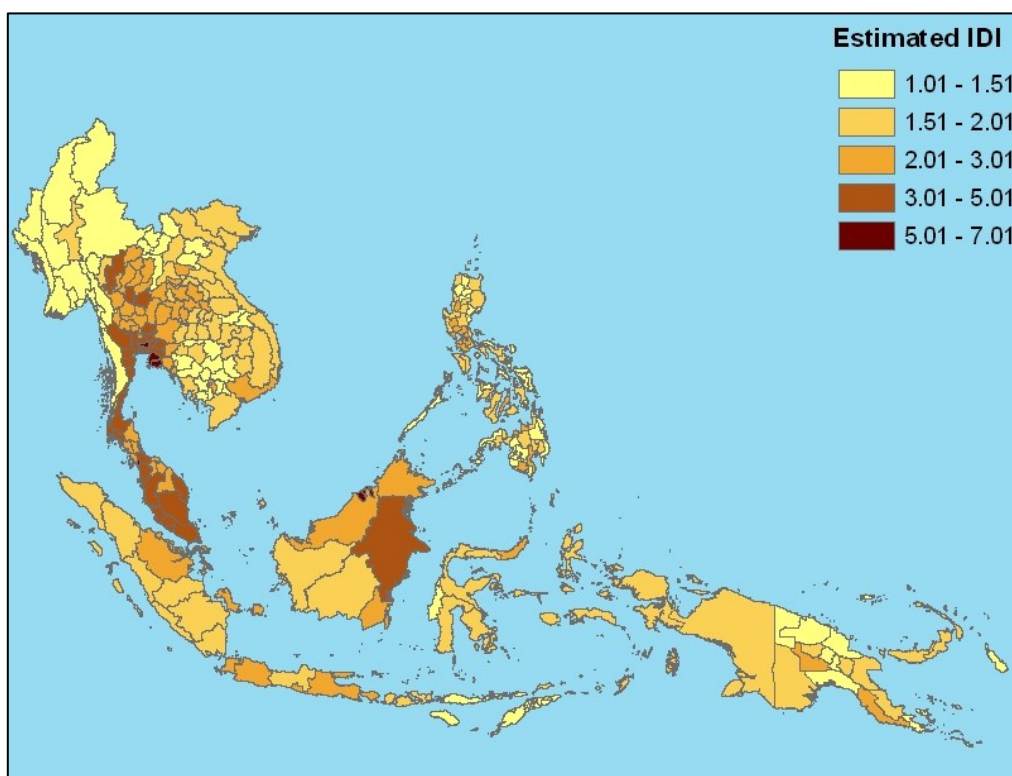


On the basis of the regression relationship between official IDI and estimated GDP per capita an attempt was made to create a global grid of IDI at 30 arc-second resolution. However, at the 30 arc-second resolution, city centers were seen to have lower GDP per capita in comparison to areas surrounding the city centers, and thus the regression relation between official IDI and estimated GDP per capita could not be employed at that spatial resolution to create the IDI grid.

Since it was not possible to create the IDI grid at the 30 arc-second resolution, the estimated IDI map was created at the sub-national level (Figure 21) and at the national level for the South-East Asian countries (South-East Asian countries was the focus because the 30th APAN meeting for which this paper was written was held in Hanoi, Vietnam in South-east Asia).

ICT promotes tremendous socio-economic development of societies, including productivity gains, development of new technologies, facilitating trade in service sectors, providing more employment in ICT-related sectors, providing enhanced flexibility for firms and workers, improving education performance, and enabling more women to participate in the employment workforce. The production of ICT maps at finer spatial resolutions from nighttime satellite images (which can be updated frequently) would facilitate government and policy makers to concentrate their resources in promoting ICT development in areas where they are lagging behind [27].

**Figure 21.** Estimated IDI map at the state level for the South-east Asian countries. (Source: adapted from [27]).



### 2.8. Use of Nighttime Lights for Measuring the Dynamics of Urban Structure

The nature of urban form and the patterns of urban development are regarded as having a fundamentally important impact on ecosystem function, ecosystem health, and sustainability [28]. Continuing studies of the dynamics of urbanization through time using nighttime lights enables

the comprehension of adverse effects of urbanization related to loss of vegetation, increase in temperatures, air and water pollution, loss of species' habitats, growth and spread of urban slums, poverty, and unemployment. Nighttime light images have added to studies of urban dynamics [29–32].

Imhoff *et al.* had used city lights data set to map urban areas of the continental United States [56]. Sutton [29] developed a “scale-adjusted” measure of urban sprawl for spatially contiguous urban areas of the conterminous United States with population of 50,000 or greater.

Zhang and Seto [30] used multi-temporal nightlight data to examine the feasibility of such data use in probing changes in urbanization at regional and global scales. They used an unsupervised classification method on the data to map urbanization dynamics in India, China, Japan, and the United States. Through their study they found out that for two-year intervals between 1992 and 2000, India constantly had higher growth rates than China, and both of these countries had higher growth rates than Japan and the U.S. These trends were in agreement with the comparative faster rates of population growth of India and China during those years. However, for the two-year intervals between 2000 and 2008, China experienced higher urban growth rates than India. They concluded that nightlight data could provide a regional and possibly global measure of the spatial and temporal changes in urbanization dynamics for countries at certain levels of economic development and whose growth are driven by growth in population.

In a latest study, Ma *et al.* [31] have investigated the long-term relations between nighttime weighted lit area and four urbanization variables—population, gross domestic product (GDP), built-up area, and electric power consumption. They used three types of regression models—linear, power-law, and exponential functions to study these long-term relationships for more than 200 prefectural level cities and municipalities for China. They established that nighttime lights could definitely serve as an explanatory indicator for these variables of urbanization dynamics at the local level. However, the quantitative models should vary with different patterns of urban development, especially for cities experiencing fast urban growth at the local scale.

Pandey *et al.* [32] used the nighttime lights and SPOT vegetation (VGT) dataset for the period 1998–2008 to extract urban areas in India employing the support vector machine (SVM) method. SVM is a semi-automated technique that enables the regional and national scale assessment of urbanization without necessitating the thresholding method for nightlights data. Different spatial metrics were calculated and analyzed state-wise, which provided information on the pattern and spread of cities and urban areas in India during those 10 years. The states of Tamil Nadu, Punjab, and Kerala, showed the highest rate of increase in urban areas. Moreover, some states showed highly aggregated patterns of urban growth while others showed a dispersed pattern.

There is a general consensus that increased urban population density is a good thing [57]. Nonetheless, this is not an absolute consensus and many regard some aspects of good urban design (e.g., biophilic urban design) to potentially be in conflict with the goals of increased urban density [58]. A recent study juxtaposing nighttime satellite imagery with radar imagery demonstrated dramatic differences between the evolution of urban structure in cities in India and China [59]. Changes to the nighttime lights were contrasted with changes to radar backscatter information. The strength of the radar backscatter was regarded as a proxy measure of increased building height. Cities in China appeared to be building up with increased urban population density whereas cities in India appeared to be growing out with larger areas of lower population density. This work represents an empirical

measure of a very fundamental difference in changing urban form that warrants greater understanding with respect to the impact these two dramatically distinct trajectories of urban growth have on human well-being. One aspect of urban structure is the extent and density of peri-urban or exurban development. This kind of development varies dramatically between the United States and Australia despite the fact that the urban areas of both countries developed extensively during the post World War II automotive era [60]. Exploration of the relationship between these diverging and unprecedented manifestations of urban form and measures of human well-being is likely to be an active research area for the near future.

### 3. Discussion

The greatest advantage of all these measures of well-being is that they provide a simple, objective, spatially explicit and globally available empirical measurement of human well-being derived solely from nighttime satellite imagery and population density. The remotely sensed nighttime images act as a satisfactory proxy variable when discrepancies in measurements of economic data like GDP, inflow of remittances, and measures of inequality such as the Gini coefficient, exist. Although in developing countries a greater percentage of economic activity is conducted in the informal economy sector, they are often excluded from formal statistics. The nighttime lights provide an alternative method for measuring the spatial distribution and magnitude of the informal economy. A great deal of economic data are made available through surveys which may be biased or influenced. In addition, these surveys often have long time intervals between administrations. Moreover, most of the data are available at the national level, and only in some cases at the sub-national level. Creating spatially explicit grids of these economic variables at 1 km<sup>2</sup> spatial resolution provides the distinctive advantage of aggregating the data to any administrative unit as desired in any study.

For example, the primary source of poverty line data in 2006 was from the World Bank. The international poverty line in purchasing power parity was specified in terms of the number of individuals living on less than \$1.08 and \$2.15 a day at 1993 international prices. A number of problems associated with the World Bank poverty line data were recognized. Not all countries conducted the survey to collect the required data and the survey repeat cycle was uncertain. The inter-comparability of the data was mired with uncertainties due to difficulties in reconciling consumption and income data, and also because of the discrepancies in the purchasing power parity estimates for individual countries. It is also likely that governments intervened and influenced the outcome of such surveys since they designed the questions, selected the areas of survey and conducted the interviews. Besides, the international poverty line can be considered to be a one-dimensional measure as it measures just the expenditure necessary to achieve the caloric intake of 2,100 calories per person per day. It ignores the multi-dimensional deprivation associated with poverty. The nighttime light images and the LandScan population data provide a globally consistent and uniform measure of poverty at the 1-km<sup>2</sup> grid level [18].

Measuring the distribution of wealth and income at national and regional scales is an interesting and challenging problem. Gini coefficients derived from Lorenz curves are a well-established method of measuring income distribution. Nonetheless, there are many shortcomings of the Gini coefficient as a measure of income or wealth distribution. For example, subsidies such as food stamps may or may not

be counted, availability of free public education may or may not be present or incorporated into these measures, and informal economic activity is difficult to measure and allocate amongst households. Official data of national level income Gini coefficients are produced by the World Bank and Central Intelligence Agency by analyzing government reported income distribution data. However, many countries do not have a well-established program to collect the required data in a consistent manner and on a repetitive basis, and in such cases comparisons between countries becomes increasingly difficult and inaccurate. Furthermore, for many countries, the data available are inadequate for the calculation of Gini coefficients, and in many cases the data, which are available, are more than a decade old. The reported Gini indices at the national level conceal the discrepancy in income distribution that exists within a country. Well-documented problems associated with the use of GDP per capita as an average measure of wealth also apply to measures of the distribution of wealth that use monetary metrics such as GDP. Using the nighttime lights and LandScan population grid to measure NLDI provides a measure of human development that completely avoids the use of monetary measures of wealth [24].

Similarly, the IEA, which has been compiling and reporting data on electrification rates since 2001 admits to having no internationally accepted definition for electric power access and no standard method for collecting such data. The agency has collected data from various sources to achieve their objective of reporting percentage of population having access to electricity. The nighttime lights provide a measure of electrification rates that is applied uniformly across the globe at a fine spatial resolution [26].

None of the approximations of human well-being using the remotely sensed nighttime images can be said to be free of errors. However, it can be assumed that a combination of several datasets having the “right” kind of measurement errors may help to reduce the error in the final product. This assumption is derived from Browning and Crossley’s study [61] in which they concluded that “it is better to have several error prone measures than one” [8].

Although artificial lighting has improved the quality of human life, and is considered as a proxy indicator of various human well-being variables in this paper, one should avoid the misinterpretation of equating light with well-being.

Exposure to light at night has distinct social, ecological, behavioral, and health consequences. The exposure disrupts the circadian system in humans and leads to deleterious physiological and psychological health consequences. Research has found that exposure to unnatural light may cause cancer due to suppressed production of melatonin; may lead to mood fluctuations and depression; and also cause obesity [62].

Light pollution has a considerable effect on the behavioral and population ecology of organisms. These effects are the result of changes in orientation, attraction or repulsion from the altered light environment, which consequently affects foraging, reproduction, migration, and communication. Ecological light pollution affects insects, amphibians, fish, birds, bats, and other animals, and can have an effect on plants by altering their day-night cycle [63].

For instance, beachfront lighting disorients hatchling sea turtles and restrains their movement to the ocean. Artificial lighting also affects the egg-laying behavior of female turtles. Artificial lighting could give rise to competition among groups of species when they forage on the same resource but have preferences for different levels of lighting. Unexpected changes in lighting can affect the prey-predator

relationships, often offering an advantage to the predator. Befuddled insects may assemble around light sources until they die of exhaustion. This in turn will reduce their biomass and population size, and the change in the relative composition of their populations will have effects further up the food chain. Artificial lighting can confuse migratory fish and birds, causing excessive energy loss and spatial obstruction to migration. Consequently, this will result in phenological changes and reduce migratory success of these fishes and birds. Artificial lighting can cause early leaf out, late leaf loss, and extended growing periods in plants, which could affect the composition of the floral community. It can also be believed that a population's genetic composition will be disturbed by light-induced selection for non-light sensitive individuals [64].

Some countries like Australia, Canada, Italy, and the UK, have taken steps to limit light pollution. Regulations are being imposed to shield outdoor lights and dimming lights during off—peak times. In February 2002, the Czech Republic became the first country to implement adoption of nation-wide lighting regulation with the passage of Protection of the Atmosphere Act [65]. These new regulations and ways of lighting may introduce bias in studies using lights to measure well-being. A region may seem to lower its light emissions because, simply, it wants to protect the night environment and improve the well-being of its citizens. By cutting the light escaping directly from fixtures towards space, the satellite will measure lower light emission while the useful light (toward the streets) will actually increase or remain unchanged.

Because of the geographical, cultural, and economic differences in lighting between countries the relation between GDP and light emissions requires further investigation. Falchi found in 1998 that, despite a factor of two difference in the per capita income of southern Italy *versus* northern Italy, the per capita light emissions were the same, as measured with DMSP data [66]. Alejandro Sanchez de Miguel found that European countries have very different lighting habits, with Spain and Italy having the highest light emissions, while more developed countries such as Germany have much lower light emissions [67].

#### 4. Conclusion

This paper has reviewed the tremendous potential of nighttime satellite imagery for providing a variety of alternative measures of human well-being. These estimates can be made on a globally consistent basis and at higher frequency intervals than the typical decadal census of the population. Moreover, since these estimates can be made as spatially disaggregated 1-km<sup>2</sup> grids, they can be aggregated to any desirable mapping unit. Cost cutting pressures in the public sector seem to be forcing much of the social science that serves the public good to rely on multiple inexpensive and uncertain measures of complex phenomena rather than single expensive measures. In the United States there is increasing pressure to eliminate major social science data sources such as the American Community Survey (ACS) [68]. On 9 May 2012 the House voted to kill the ACS. In light of the growing threats to the availability of good social science data, the kinds of proxy measures described here are appealing because they have lower costs of acquisition, are available globally, and appear to have validity. The nighttime lights data provided by the DMSP-OLS do have significant observational shortcomings including coarse spatial and spectral resolution and lack of onboard calibration. Recently, the Visible Infrared Imaging Radiometer Suite (VIIRS) flying on the Suomi National

Polar-orbiting partnership (NPP) between NASA and NOAA since October 2011 has provided data of higher spatial resolution (742 m) and spectral resolution (22 spectral bands covering visible, near-infrared, and thermal infrared regions). The use of high resolution nighttime data from VIIRS will definitely improve the capabilities of nighttime observation of the earth and to the related ways these nighttime lights images can inform our understanding and measurement of human well-being.

### Conflicts of Interest

The authors declare no conflict of interest.

### References

1. Bergh, J.C.J.M. The GDP paradox. *J. Econ. Psychol.* **2009**, *30*, 117–135.
2. Elvidge, C.D.; Baugh, K.E.; Kihn, E.A.; Koehl, H.W.; Davis, E.R.; Davis, C.W. Relation between satellites observed visible near-infrared emissions, population, economic activity and power consumption. *Int. J. Remote Sens.* **1997**, *18*, 1373–1379.
3. Doll, C.N.H.; Muller, J.P.; Elvidge, C.D. Nighttime imagery as a tool for global mapping of socioeconomic parameters and greenhouse gas emissions. *Ambio* **2000**, *29*, 157–162.
4. Sutton, P.C.; Costanza, R. Global estimates of market and non-market values derived from nighttime satellite imagery, land cover, and ecosystem service evaluation. *Ecol. Econ.* **2002**, *41*, 509–527.
5. Ebener, S.; Murray, C.; Tandon, A.; Elvidge, C.D. From wealth to health: Modeling the distribution of income per capita at the subnational level using nighttime light imagery. *Int. J. Health Geogr.* **2005**, *4*, 1–17.
6. Doll, C.N.H.; Muller, J.P.; Morley, J.G. Mapping regional economic activity from night-time light satellite imagery. *Ecol. Econ.* **2006**, *57*, 75–92.
7. Sutton, P.C.; Elvidge, C.D.; Ghosh, T. Estimation of gross domestic product at sub-national scales using nighttime satellite imagery. *Int. J. Ecol. Econ. Stat.* **2007**, *8*, 5–21.
8. Ghosh, T.; Powell, R.; Elvidge, C.D.; Baugh, K.E.; Sutton, P.C.; Anderson, S. Shedding light on the global distribution of economic activity. *Open Geogr. J.* **2010**, *3*, 147–160.
9. Chen, X.; Nordhaus, W.D. Using luminosity data as a proxy for economic statistics. *Proc. Natl. Acad. Sci. USA.* **2010**, *108*, 8589–8594.
10. Bhandari, L.; Roychowdhury, K. Night lights and economic activity in India: A study using DMSP-OLS night time images. *Proc. Asia Pac. Adv. Netw.* **2011**, *32*, 218–236.
11. Chaturvedi, M.; Ghosh, T.; Bhandari, L. Assessing income distribution at the district level for India using nighttime satellite imagery. *Proc. Asia Pac. Adv. Netw.* **2011**, *32*, 192–217.
12. Henderson, J.V.; Storeygard, A.; Weil, D.N. Measuring economic growth from outer space. *Am. Econ. Rev.* **2012**, *102*, 994–1028.
13. Propastin, P.; Kappas, M. Assessing satellite-observed nighttime lights for monitoring socio-economic parameters in the Republic of Kazakhstan. *Gisci. Remote Sens.* **2012**, *49*, 538–557.
14. Xiangdi, H.; Yi, Z.; Shixin, W.; Ryu, L.; Yao, Y. GDP spatialization in China based on nighttime imagery. *Geo-Inf Sci.* **2012**, *V14*, 128–136.

15. Pestalozzi, N.; Cauwels, P.; Sornette, D. *Dynamics and Spatial Distribution of Global Nighttime Lights*; Swiss Finance Institute Research Paper No. 13-02. Available online: [http://papers.ssrn.com/sol3/papers.cfm?abstract\\_id=2237410](http://papers.ssrn.com/sol3/papers.cfm?abstract_id=2237410) (accessed on 27 September 2013).
16. Satoru, K.; Souknilanh, K.; Toshihiro, K. Myanmar Economy Viewed at Night. IDE Discussion Papers, Policy Review on Myanmar Economy No. 5. Available online: <http://www.ide.go.jp/English/Publish/Download/Brc/PolicyReview/05.html> (accessed on 27 September 2013).
17. Mellander, C.; Stolarick, K.; Matheson, Z.; Lobo, J. Night-Time Light Data: A Good Proxy Measure for Economic Activity? CESIS Electronic Working Paper Series, The Royal Institute of Technology, Centre of Excellence for Science and Innovation Studies (CESIS). Available online: <http://www.kth.se/dokument/itm/cesis/cesiswp315.pdf> (accessed on 27 September 2013).
18. Elvidge, C.D.; Sutton, P.C.; Ghosh, T.; Tuttle, B.T.; Baugh, K.E.; Bhaduri, B. A global poverty map derived from satellite data. *Comput. Geosci.* **2009**, *35*, 1652–1660.
19. Noor, A.M.; Alegana, V.A.; Gething, P.W.; Tatem, A.J.; Snow, R.W. Using remotely sensed night-time light as a proxy for poverty in Africa. *Popul. Health Metr.* **2008**, *6*, 5.
20. Weng, W.; Cheng, H.; Zhang, L. Poverty assessment using DMSP/OLS night-time light satellite imagery at a provincial scale in China. *Adv. Space Res.* **2012**, *49*, 1253–1264.
21. World Bank. *DC Big Data Exploration Final Report*; World Bank Group Finances: Washington, DC, USA, 2013. Available online: [http://www.scribd.com/doc/142012481/DC-Big-Data-Exploration-Final-Report?cid=CTR\\_TwitterWBopenfinances\\_D\\_EXT](http://www.scribd.com/doc/142012481/DC-Big-Data-Exploration-Final-Report?cid=CTR_TwitterWBopenfinances_D_EXT) (accessed on 27 September 2013).
22. Kubizewski, I.; Costanza, R.; Franco, C.; Lawn, P.; Talberth, J.; Jackson, T.; Aylmer, C. Beyond GDP: Measuring and achieving global genuine progress. *Ecol. Econ.* **2013**, *93*, 57–68.
23. Ghosh, T.; Anderson, S.; Powell, R.L.; Sutton, P.C.; Elvidge, C.D. Estimation of Mexico's informal economy and remittances using nighttime imagery. *Remote Sens.* **2009**, *1*, 418–444.
24. Elvidge, C.D.; Baugh, K.E.; Anderson, S.J.; Sutton, P.C.; Ghosh, T. The Night Light Development Index (NLDI): A spatially explicit measure of human development from satellite Data. *Soc. Geogr.* **2012**, *7*, 23–35.
25. Sutton, P.C.; Anderson, S.J.; Tuttle, B.J.; Morse, L. The real wealth of nations. *Ecol. Indic.* **2012**, *16*, 11–22.
26. Elvidge, C.D.; Baugh, K.E.; Sutton, P.C.; Bhaduri, B.; Tuttle, B.; Ghosh, T.; Ziskin, D.; Erwin, E.H. Who's in the Dark—Satellite Based Estimates of Electrification Rates. In *Urban Remote Sensing: Monitoring, Synthesis and Modeling in the Urban Environment*, 1st ed.; Yang, X.J., Ed.; Willey-Blackwell: Chichester, West Sussex, UK, 2011; pp. 211–224.
27. Ghosh, T.; Elvidge, C.D.; Sutton, P.C.; Baugh, K.E.; Ziskin, D. Estimating the Information and Technology Development Index (IDI) Using Nighttime Satellite Imagery. In Proceedings of the Asia Pacific Advanced Network, Hanoi, Vietnam, 9–13 August 2010.
28. Alberti, M. The effects of urban patterns on ecosystem function. *Int. Reg. Sci. Rev.* **2005**, *28*, 168–192.
29. Sutton, P.C. A scale-adjusted measure of “urban-sprawl” using nighttime satellite imagery. *Remote Sens. Environ.* **2003**, *86*, 353–369.
30. Zhang, Q.; Seto, K.C. Mapping urbanization dynamics at regional and global scales using multi-temporal DMSP/OLS nighttime light data. *Remote Sens. Environ.* **2011**, *115*, 2320–2329.

31. Ma, T.; Zhou, C.; Pei, T.; Haynie, S.; Fan, J. Quantitative estimation of urbanization dynamics using time series of DMSP/OLS nighttime light data: A comparative case study from China's cities. *Remote Sens. Environ.* **2012**, *124*, 99–107.
32. Pandey, B.; Joshi, P.K.; Seto, K.C. Monitoring urbanization dynamics in India using DMSP/OLS nighttime lights and SPOT-VGT data. *Int. J. Appl. Earth Obs.* **2013**, *23*, 49–61.
33. Baugh, K.; Elvidge, C.D.; Ghosh, T.; Ziskin, D. Development of a 2009 Stable Lights Product Using DMSP-OLS Data. In Proceedings of the Asia-Pacific Advanced Network 30, Hanoi, Vietnam, 9–13 August 2010; pp. 114–130.
34. Stable Lights Images, 1992–2012, Earth Observation Group. Available online: <http://ngdc.noaa.gov/eog/dmsp/downloadV4composites.html> (accessed on 27 September 2013).
35. Ziskin, D.; Baugh, K.; Hsu, F.C.; Ghosh, T.; Elvidge, C.D. Methods Used for the 2006 Radiance Lights. In Proceedings of the Asia-Pacific Advanced Network 30, Hanoi, Vietnam, 9–13 August 2010.
36. Radiance-Calibrated Image, 2006, Earth Observation Group. Available online: [http://ngdc.noaa.gov/eog/dmsp/download\\_radcal.html](http://ngdc.noaa.gov/eog/dmsp/download_radcal.html) (accessed on 27 September 2013).
37. LandScan, Oak Ridge National Laboratory. Available online: <http://www.ornl.gov/sci/landscan/> (accessed on 27 September 2013).
38. Schneider, F. Size and Measurement of the Informal Economy in 110 Countries around the World. Presented at the Workshop of Australian National Tax Center, ANU, Canberra, Australia, 17 July 2002.
39. Schneider, F. *The Size of the Shadow Economy in 21 OECD Countries (in Percent of "Official" GDP) Using the MIMIC and Currency Demand Approach: From 1989/90 to 2009*; Johannes Kepler Universitat: Linz, Austria, 2009.
40. Schneider, F. *The Size of the Shadow Economy for 25 Transition Countries over 1999/00 to 2006/07: What Do We Know?* Johannes Kepler Universitat: Linz, Austria, 2009.
41. World Bank. *World Development Indicators*; World Bank: Washington, DC, USA, 2006.
42. Nordbeck, S. *The Law of Allometric Growth. Michigan Inter-University Community of Mathematical Geographers*; Paper No.7; Department of Geography, University of Michigan: Ann Arbor, MI, USA, 1965.
43. McTague, J. Going Underground: America's Shadow Economy. *FrontPage Magazine*, 6 January 2005. Available online: <http://www.frontpagemag.com/readArticle.aspx?ARTID=10024> (accessed on 12 November 2013).
44. Harvard Business Review—Informal Economy. [http://blogs.hbr.org/cs/2012/01/the\\_candy\\_man\\_in\\_america.html](http://blogs.hbr.org/cs/2012/01/the_candy_man_in_america.html) (accessed on 12 November 2013).
45. Pickett, K.; Wilkinson, R. *The Spirit Level: Why Greater Equality Makes Societies Stronger*; Bloomsbury Press: New York, NY, USA, 2010.
46. Wackernagel, M.; Rees, W.E. *Our Ecological Footprint: Reducing Human Impact on the Earth Sharing Nature's Interest*; New Society Publishers: Gabriola Island, BC, Canada, 1996.
47. Elvidge, C.D.; Tuttle, B.T.; Sutton, P.C.; Baugh, K.E.; Howard, A.T.; Milesi, C.; Bhaduri, B.L.; Nemani, R. Global distribution and density of constructed impervious surfaces. *Sensors* **2007**, *7*, 1962–1976.

48. Imhoff, M.L.; Bounoua, L.; Ricketts, T.; Loucks, C.; Harriss, R.; Lawrence, W.T. Global patterns in human consumption of net primary production. *Nature* **2004**, *429*, 870–873.
49. *2006 Annual Report*; Wackernagel, M., Ed.; Global Footprint Network: Oakland, CA, USA, 2006.
50. International Energy Agency. *World Energy Outlook*; OECD, IEA: Paris, France, 2002. Available online: [http://www.worldenergyoutlook.org/media/weowebiste/2008-1994/weo2002\\_part1.pdf](http://www.worldenergyoutlook.org/media/weowebiste/2008-1994/weo2002_part1.pdf) (accessed on 27 September 2013).
51. International Energy Agency. Appendix to Chapter 10: Electrification Tables. In *World Energy Outlook*; IEA: Paris, France, 2006.
52. United Nations Development Programme. Electrification Rate by Country 2007/2008. Available online: [http://www.photius.com/rankings/electrification\\_by\\_country\\_2007\\_2008.html](http://www.photius.com/rankings/electrification_by_country_2007_2008.html) (accessed on 27 September 2013).
53. Elvidge, C.D.; Ziskin, D.; Baugh, K.E.; Tuttle, B.T.; Ghosh, T.; Pack, D.W.; Erwin, E.H.; Zhizhin, M. A fifteen year record of global natural gas flaring derived from satellite data. *Energies* **2009**, *2*, 595–622.
54. Kiran Chand, T.R.; Badarinath, K.V.S.; Elvidge, C.D.; Tuttle, B.T. Spatial characterization of electrical power consumption patterns over India using temporal DMSP-OLS night-time satellite data. *Int. J. Remote Sens.* **2009**, *30*, 647–661.
55. International Telecommunication Union. *Measuring the Information Society*, Version 1.01; International Telecommunication Union: Geneva, Switzerland, 2010. Available online: [http://www.itu.int/ITU-D/ict/publications/idi/material/2010/MIS\\_2010\\_without\\_annex\\_4-e.pdf](http://www.itu.int/ITU-D/ict/publications/idi/material/2010/MIS_2010_without_annex_4-e.pdf) (accessed on 27 September 2013).
56. Imhoff, M.L.; Lawrence, W.T.; Stutzer, D.C.; Elvidge, C.D. A technique for using composite DMSP/OLS “city lights” satellite data to map urban area. *Remote Sens. Environ.* **1997**, *61*, 361–370.
57. United States Environmental Protection Agency. *Our Built and Natural Environments: A Technical Review of the Interactions Between Land Use, Transportation, and Environmental Quality*; United States Environmental Protection Agency: Washington, DC, USA, 2001. Available online: <http://www.epa.gov/smartgrowth/pdf/built.pdf> (accessed on 27 September 2013).
58. Loukaitou-Sideris, A. Addressing the challenges of urban landscapes: Normative goals for urban design. *J. Urban Des.* **2012**, *17*, 467–484.
59. Froliking, S.; Milliman, T.; Seto, K.C.; Friedl, M.A. A global fingerprint of macro-scale changes in urban structure from 1999 to 2009. *Environ. Res. Lett.* **2013**, *8*, 1–10.
60. Sutton, P.C.; Fildes, S.; Forster, C.; Ghosh, T.; Goetz, A. Darkness on the edge of town: Mapping urban and peri-urban Australia using nighttime satellite imagery. *Prof. Geogr.* **2010**, *62*, 119–133.
61. Browning, M.; Crossley, T. Are two cheap, noisy measures better than one expensive, accurate one? *Am. Econ. Rev.* **2009**, *99*, 99–108.
62. Fonken, L.K.; Nelson, R.J. Illuminating the deleterious effects of light at night. *PMC F1000 Med. Rep.* **2011**, *3*, 18.
63. Longcore, T.; Rich, C. Ecological light pollution. *Front. Ecol. Environ.* **2004**, *2*, 191–198.
64. Holker, F.; Wolter, C.; Elizabeth, P.K.; Tockner, K. Light pollution as a biodiversity threat. *Trends Ecol. Evol.* **2010**, *25*, 681–682.

65. Shi, J. *Reducing Artificial Nighttime Lights Pollution and Its Impacts*. Geographic Strategies Group, Office of Air Quality Planning and Standards; Environmental Protection Agency: Raleigh, NC, USA, 2010. Available online: [http://www.trianglealumni.org/mcrol/EPA-NNEMS\\_Light\\_Pollution\\_Final.pdf](http://www.trianglealumni.org/mcrol/EPA-NNEMS_Light_Pollution_Final.pdf) (accessed on 27 September 2013).
66. Falchi, F.; Cinzano, P. Maps of Artificial Sky Brightness and Upward Emission in Italy from Satellite Measurements. In *Measuring and Modelling Light Pollution*; Cinzano, P., Ed.; Journal of Italian Astronomical Society: Palermo, Italy, 2000; pp. 139–152. Available online: <http://www.lightpollution.it/cinzano/memorie/memsait.pdf> (accessed on 27 September 2013).
67. Sánchez de Miguel, A. Differential Photometric Study of the European Light Emission to the Space—A common Heritage. In *Starlight A Common Heritage*; Marin, C., Jafari, J., Eds.; Starlight Initiative, IAC: Canary Islands, Spain, 2007; pp. 379–383. Available online: <http://www.starlight2007.net/pdf/StarlightCommonHeritage.pdf> (accessed on 27 September 2013).
68. Killing the American Community Survey Blinds Business. Available online: <http://www.businessweek.com/articles/2012-05-10/killing-the-american-community-survey-blinds-business> (accessed on 27 September 2013).

© 2013 by the authors; licensee MDPI, Basel, Switzerland. This article is an open access article distributed under the terms and conditions of the Creative Commons Attribution license (<http://creativecommons.org/licenses/by/3.0/>).